

AD-A100 153

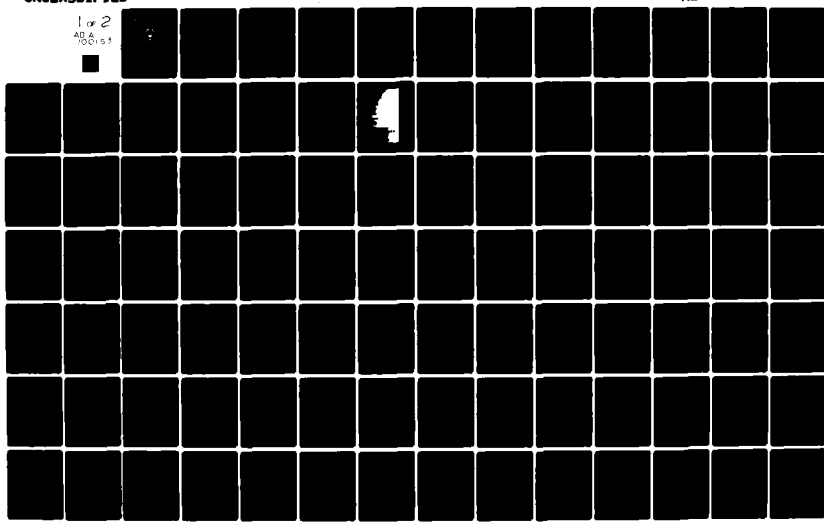
NAVAL POSTGRADUATE SCHOOL MONTEREY CA
DATA ASSIMILATION IN A ONE-DIMENSIONAL OCEANIC MIXED LAYER MODEL--ETC(U)
DEC 80 L L WARRENFELTZ

F/6 8/10

NL

UNCLASSIFIED

1 of 2
ADA
100-153



LEVEL

2

NAVAL POSTGRADUATE SCHOOL

Monterey, California

60
120
150
180
210
240
270
300
330
360
390
420
450
480
510
540
570
600
630
660
690
720
750
780
810
840
870
900
930
960
990
1020
1050
1080
1110
1140
1170
1200
1230
1260
1290
1320
1350
1380
1410
1440
1470
1500
1530
1560
1590
1620
1650
1680
1710
1740
1770
1800
1830
1860
1890
1920
1950
1980
2010
2040
2070
2100
2130
2160
2190
2220
2250
2280
2310
2340
2370
2400
2430
2460
2490
2520
2550
2580
2610
2640
2670
2700
2730
2760
2790
2820
2850
2880
2910
2940
2970
3000
3030
3060
3090
3120
3150
3180
3210
3240
3270
3300
3330
3360
3390
3420
3450
3480
3510
3540
3570
3600
3630
3660
3690
3720
3750
3780
3810
3840
3870
3900
3930
3960
3990
4020
4050
4080
4110
4140
4170
4200
4230
4260
4290
4320
4350
4380
4410
4440
4470
4500
4530
4560
4590
4620
4650
4680
4710
4740
4770
4800
4830
4860
4890
4920
4950
4980
5010
5040
5070
5100
5130
5160
5190
5220
5250
5280
5310
5340
5370
5400
5430
5460
5490
5520
5550
5580
5610
5640
5670
5700
5730
5760
5790
5820
5850
5880
5910
5940
5970
5990
6020
6050
6080
6110
6140
6170
6200
6230
6260
6290
6320
6350
6380
6410
6440
6470
6500
6530
6560
6590
6620
6650
6680
6710
6740
6770
6800
6830
6860
6890
6920
6950
6980
7010
7040
7070
7100
7130
7160
7190
7220
7250
7280
7310
7340
7370
7400
7430
7460
7490
7520
7550
7580
7610
7640
7670
7700
7730
7760
7790
7820
7850
7880
7910
7940
7970
8000
8030
8060
8090
8120
8150
8180
8210
8240
8270
8300
8330
8360
8390
8420
8450
8480
8510
8540
8570
8600
8630
8660
8690
8720
8750
8780
8810
8840
8870
8900
8930
8960
8990
9020
9050
9080
9110
9140
9170
9200
9230
9260
9290
9320
9350
9380
9410
9440
9470
9500
9530
9560
9590
9620
9650
9680
9710
9740
9770
9800
9830
9860
9890
9920
9950
9980
10010
10040
10070
10100
10130
10160
10190
10220
10250
10280
10310
10340
10370
10400
10430
10460
10490
10520
10550
10580
10610
10640
10670
10700
10730
10760
10790
10820
10850
10880
10910
10940
10970
11000
11030
11060
11090
11120
11150
11180
11210
11240
11270
11300
11330
11360
11390
11420
11450
11480
11510
11540
11570
11600
11630
11660
11690
11720
11750
11780
11810
11840
11870
11900
11930
11960
11990
12020
12050
12080
12110
12140
12170
12200
12230
12260
12290
12320
12350
12380
12410
12440
12470
12500
12530
12560
12590
12620
12650
12680
12710
12740
12770
12800
12830
12860
12890
12920
12950
12980
13010
13040
13070
13100
13130
13160
13190
13220
13250
13280
13310
13340
13370
13400
13430
13460
13490
13520
13550
13580
13610
13640
13670
13700
13730
13760
13790
13820
13850
13880
13910
13940
13970
14000
14030
14060
14090
14120
14150
14180
14210
14240
14270
14300
14330
14360
14390
14420
14450
14480
14510
14540
14570
14600
14630
14660
14690
14720
14750
14780
14810
14840
14870
14900
14930
14960
14990
15020
15050
15080
15110
15140
15170
15200
15230
15260
15290
15320
15350
15380
15410
15440
15470
15500
15530
15560
15590
15620
15650
15680
15710
15740
15770
15800
15830
15860
15890
15920
15950
15980
16010
16040
16070
16100
16130
16160
16190
16220
16250
16280
16310
16340
16370
16400
16430
16460
16490
16520
16550
16580
16610
16640
16670
16700
16730
16760
16790
16820
16850
16880
16910
16940
16970
17000
17030
17060
17090
17120
17150
17180
17210
17240
17270
17300
17330
17360
17390
17420
17450
17480
17510
17540
17570
17600
17630
17660
17690
17720
17750
17780
17810
17840
17870
17900
17930
17960
17990
18020
18050
18080
18110
18140
18170
18200
18230
18260
18290
18320
18350
18380
18410
18440
18470
18500
18530
18560
18590
18620
18650
18680
18710
18740
18770
18800
18830
18860
18890
18920
18950
18980
19010
19040
19070
19100
19130
19160
19190
19220
19250
19280
19310
19340
19370
19400
19430
19460
19490
19520
19550
19580
19610
19640
19670
19700
19730
19760
19790
19820
19850
19880
19910
19940
19970
20000
20030
20060
20090
20120
20150
20180
20210
20240
20270
20300
20330
20360
20390
20420
20450
20480
20510
20540
20570
20600
20630
20660
20690
20720
20750
20780
20810
20840
20870
20900
20930
20960
20990
21020
21050
21080
21110
21140
21170
21200
21230
21260
21290
21320
21350
21380
21410
21440
21470
21500
21530
21560
21590
21620
21650
21680
21710
21740
21770
21800
21830
21860
21890
21920
21950
21980
22010
22040
22070
22100
22130
22160
22190
22220
22250
22280
22310
22340
22370
22400
22430
22460
22490
22520
22550
22580
22610
22640
22670
22700
22730
22760
22790
22820
22850
22880
22910
22940
22970
23000
23030
23060
23090
23120
23150
23180
23210
23240
23270
23300
23330
23360
23390
23420
23450
23480
23510
23540
23570
23600
23630
23660
23690
23720
23750
23780
23810
23840
23870
23900
23930
23960
23990
24020
24050
24080
24110
24140
24170
24200
24230
24260
24290
24320
24350
24380
24410
24440
24470
24500
24530
24560
24590
24620
24650
24680
24710
24740
24770
24800
24830
24860
24890
24920
24950
24980
25010
25040
25070
25100
25130
25160
25190
25220
25250
25280
25310
25340
25370
25400
25430
25460
25490
25520
25550
25580
25610
25640
25670
25700
25730
25760
25790
25820
25850
25880
25910
25940
25970
26000
26030
26060
26090
26120
26150
26180
26210
26240
26270
26300
26330
26360
26390
26420
26450
26480
26510
26540
26570
26600
26630
26660
26690
26720
26750
26780
26810
26840
26870
26900
26930
26960
26990
27020
27050
27080
27110
27140
27170
27200
27230
27260
27290
27320
27350
27380
27410
27440
27470
27500
27530
27560
27590
27620
27650
27680
27710
27740
27770
27800
27830
27860
27890
27920
27950
27980
28010
28040
28070
28100
28130
28160
28190
28220
28250
28280
28310
28340
28370
28400
28430
28460
28490
28520
28550
28580
28610
28640
28670
28700
28730
28760
28790
28820
28850
28880
28910
28940
28970
29000
29030
29060
29090
29120
29150
29180
29210
29240
29270
29300
29330
29360
29390
29420
29450
29480
29510
29540
29570
29600
29630
29660
29690
29720
29750
29780
29810
29840
29870
29900
29930
29960
29990
30020
30050
30080
30110
30140
30170
30200
30230
30260
30290
30320
30350
30380
30410
30440
30470
30500
30530
30560
30590
30620
30650
30680
30710
30740
30770
30800
30830
30860
30890
30920
30950
30980
31010
31040
31070
31100
31130
31160
31190
31220
31250
31280
31310
31340
31370
31400
31430
31460
31490
31520
31550
31580
31610
31640
31670
31700
31730
31760
31790
31820
31850
31880
31910
31940
31970
32000
32030
32060
32090
32120
32150
32180
32210
32240
32270
32300
32330
32360
32390
32420
32450
32480
32510
32540
32570
32600
32630
32660
32690
32720
32750
32780
32810
32840
32870
32900
32930
32960
32990
33020
33050
33080
33110
33140
33170
33200
33230
33260
33290
33320
33350
33380
33410
33440
33470
33500
33530
33560
33590
33620
33650
33680
33710
33740
33770
33800
33830
33860
33890
33920
33950
33980
34010
34040
34070
34100
34130
34160
34190
34220
34250
34280
34310
34340
34370
34400
34430
34460
34490
34520
34550
34580
34610
34640
34670
34700
34730
34760
34790
34820
34850
34880
34910
34940
34970
35000
35030
35060
35090
35120
35150
35180
35210
35240
35270
35300
35330
35360
35390
35420
35450
35480
35510
35540
35570
35600
35630
35660
35690
35720
35750
35780
35810
35840
35870
35900
35930
35960
35990
36020
36050
36080
36110
36140
36170
36200
36230
36260
36290
36320
36350
36380
36410
36440
36470
36500
36530
36560
36590
36620
36650
36680
36710
36740
36770
36800
36830
36860
36890
36920
36950
36980
37010
37040
37070
37100
37130
37160
37190
37220
37250
37280
37310
37340
37370
37400
37430
37460
37490
37520
37550
37580
37610
37640
37670
37700
37730
37760
37790
37820
37850
37880
37910
37940
37970
38000
38030
38060
38090
38120
38150
38180
38210
38240
38270
38300
38330
38360
38390
38420
38450
38480
38510
38540
38570
38600
38630
38660
38690
38720
38750
38780
38810
38840
38870
38900
38930
38960
38990
39020
39050
39080
39110
39140
39170
39200
39230
39260
39290
39320
39350
39380
39410
39440
39470
39500
39530
39560
39590
39620
39650
39680
39710
39740
39770
39800
39830
39860
39890
39920
39950
39980
40010
40040
40070
40100
40130
40160
40190
40220
40250
40280
40310
40340
40370
40400
40430
40460
40490
40520
40550
40580
40610
40640
40670
40700
40730
40760
40790
40820
40850
40880
40910
40940
40970
41000
41030
41060
41090
41120
41150
41180
41210
41240
41270
41300
41330
41360
41390
41420
41450
41480
41510
41540
41570
41600
41630
41660
41690
41720
41750
41780
41810
41840
41870
41900
41930
41960
41990
42020
42050
42080
42110
42140
42170
42200
42230
42260
42290
42320
42350
42380
42410
42440
42470
42500
42530
42560
42590
42620
42650
42680
42710
42740
42770
42800
42830
42860
42890
42920
42950
42980
43010
43040
43070
43100
43130
43160
43190
43220
43250
43280
43310
43340
43370
43400
43430
43460
43490
43520
43550
43580
43610
43640
43670
43700
43730
43760
43790
43820
43850
43880
43910
43940
43970
44000
44030
44060
44090
44120
44150
44180
44210
44240
44270
44300
44330
44360
44390
44420
44450
44480
44510
44540
44570
44600
44630
44660
44690
44720
44750
44780
44810
44840
44870
44900
44930
44960
44990
45020
45050
45080
45110
45140
45170
45200
45230
45260
45290
45320
45350
45380
45410
45440
45470
45500
45530
45560
45590
45620
45650
45680
45710
45740
45770
45800
45830
45860
45890
45920
45950
45980
46010
46040
46070
46100
46130
46160
46190
46220
46250
46280
46310
46340
46370
46400
46430
46460
46490
46520
46550
46580
46610
46640
46670
46700
46730
46760
46790
46820
46850
46880
46910
46940
46970
47000
47030
47060
47090
47120
47150
47180
47210
47240
47270
47300
47330
47360
47390
47420
47450
47480
47510
47540
47570
47600
47630
47660
47690
47720
47750
47780
47810
47840
47870
47900
47930
47960
47990
48020
48050
48080
48110
48140
48170
48200
48230
48260
48290
48320
48350
48380
48410
48440
48470
48500
48530
48560
48590
48620
48650
48680
48710
48740
48770
48800
48830
48860
48890
48920
48950
48980
49010
49040
49070
49100
49130
49160
49190
49220
49250
49280
49310
49340
49370
49400
49430
49460
49490
49520
49550
49580
49610
49640
49670
49700
49730
49760
49790
49820
49850
49880
49910
49940
49970
50000
50030
50060
50090
50120
50150
50180
50210
50240
50270
50300
50330
50360
50390
50420
50450
50480
50510
50540
50570
50600
50630
50660
50690
50720
50750
50780
50810
50840
50870
50900
50930
50960
50990
51020
51050
51080
51110
51140
51170
51200
51230
51260
51290
51320
51350
51380
51410
51440
51470
51500
51530
51560
51590
51620
51650
51680
51710
51740
51770
51800
51830
51860
51890
51920
51950
51980
52010
52040
52070
52100
52130
52160
52190
52220
52250
52280
52310
52340
52370
52400
52430
52460
52490
52520
52550
52580
52610
52640
52670
52700
52730
52760
52790
52820
52850
52880
52910
52940
52970
53000
53030
53060
53090
53120
53150
53180
53210
53240
53270
53300
53330
53360
53390
53420
53450
53480
53510
53540
53570
53600
53630
53660
53690
53720
53750
53780
53810
53840
53870
53900
53930
53960
53990
54020
54050
54080
54110
54140
54170
54200
54230
54260
54290
54320
54350
54380
54410
54440
54470
54500
54530
54560



THESIS

DATA ASSIMILATION IN A ONE-DIMENSIONAL OCEANIC MIXED LAYER MODEL

by

Larry Lee Warrenfeltz

December 1980

Thesis Advisor:

R. L. Elsberry

Approved for public release; distribution unlimited.

DATA FILE COPY

813 43334

UNCLASSIFIED

SECURITY CLASSIFICATION OF THIS PAGE (When Data Entered)

REPORT DOCUMENTATION PAGE		READ INSTRUCTIONS BEFORE COMPLETING FORM
1. REPORT NUMBER	2. GOVT ACCESSION NO.	3. RECIPIENT'S CATALOG NUMBER
		AD-A100 153
4. TITLE (and Subtitle) Data Assimilation in a One-Dimensional Oceanic Mixed Layer Model		5. TYPE OF REPORT & PERIOD COVERED Master's Thesis; December 1980
7. AUTHOR(s) Larry Lee Warrenfeltz		6. PERFORMING ORG. REPORT NUMBER
8. PERFORMING ORGANIZATION NAME AND ADDRESS Naval Postgraduate School Monterey, California 93940		10. PROGRAM ELEMENT, PROJECT, TASK AREA & WORK UNIT NUMBERS
11. CONTROLLING OFFICE NAME AND ADDRESS Naval Postgraduate School Monterey, California 93940		12. REPORT DATE December 1980
14. MONITORING AGENCY NAME & ADDRESS (if different from Controlling Office)		13. NUMBER OF PAGES 110
		15. SECURITY CLASS. (of this report) Unclassified
		16a. DECLASSIFICATION/DOWNGRADING SCHEDULE
16. DISTRIBUTION STATEMENT (of this Report) Approved for public release; distribution unlimited.		
17. DISTRIBUTION STATEMENT (of the abstract entered in Block 20, if different from Report)		
18. SUPPLEMENTARY NOTES		
19. KEY WORDS (Continue on reverse side if necessary and identify by block number) 1-D ocean modeling, oceanic mixed layer, upper ocean prediction, oceanic planetary boundary layer		
20. ABSTRACT (Continue on reverse side if necessary and identify by block number) Requirements for an operational oceanic mixed layer model are discussed. Data assimilation comparisons in oceanic modeling studies and in numerical weather prediction are made. A method for assimilating data in one-dimensional oceanic models is described. The Garwood One-Dimensional Oceanic Planetary Boundary Layer Model was modified for insertion of temperature profiles during model integration. The		

UNCLASSIFIED

SECURITY CLASSIFICATION OF THIS PAGE/When Data Entered

(20. ABSTRACT CONTINUED)

sensitivity of the model to insertions of erroneous temperature data is tested. Insertions were made in winter, summer, and during the spring transition.

The hypothesis was formulated that forecasts made by the Garwood model could be improved by using all available past temperature information. Simulated temperature "history" profiles were created for 14 years between 1953 and 1969. The experiments showed improvement in the 15-day forecasts when 5, 15, or 30 history profiles were included in the initialization of the model. A gross-error check to eliminate erroneous profiles further increased forecast accuracy.

CH

Accession For

NTIS GRA&I	<input checked="" type="checkbox"/>
PUB TAB	<input type="checkbox"/>
Unpublished	<input type="checkbox"/>
Justification	<input type="checkbox"/>
Distribution	
Availability Codes	
Date	

P

Approved for public release; distribution unlimited.

Data Assimilation in a
One-Dimensional Oceanic Mixed Layer Model

by

Larry Lee Warrenfeltz
Lieutenant, United States Navy
B.S., United States Naval Academy, 1975

Submitted in partial fulfillment of the
requirements for the degree of

MASTER OF SCIENCE IN METEOROLOGY AND OCEANOGRAPHY

from the

NAVAL POSTGRADUATE SCHOOL
December 1980

Author

Approved by:

Larry L. Warrenfeltz

Russell L. Eldenby

Thesis Advisor

Roland W. Donwood Jr

Second Reader

Winfred J. Marshall

Chairman, Department of Meteorology

William M. Tolles

Dean of Science and Engineering

ABSTRACT

Requirements for an operational oceanic mixed layer model are discussed. Data assimilation comparisons in oceanic modeling studies and in numerical weather prediction are made. A method for assimilating data in one-dimensional oceanic models is described. The Garwood One-Dimensional Oceanic Planetary Boundary Layer Model was modified for insertion of temperature profiles during model integration. The sensitivity of the model to insertions of erroneous temperature data is tested. Insertions were made in winter, summer, and during the spring transition.

The hypothesis was formulated that forecasts made by the Garwood model could be improved by using all available past temperature information. Simulated temperature "history" profiles were created for 14 years between 1953 and 1969. The experiments showed improvement in the 15-day forecasts when 5, 15, or 30 history profiles were included in the initialization of the model. A gross-error check to eliminate erroneous profiles further increased forecast accuracy.

TABLE OF CONTENTS

LIST OF TABLES -----	7
LIST OF FIGURES -----	8
ACKNOWLEDGMENTS -----	11
I. INTRODUCTION -----	12
A. THE OCEANIC PLANETARY BOUNDARY LAYER -----	12
B. REQUIREMENTS FOR AN OPERATIONAL OPBL PREDICTION MODEL -----	15
C. DESCRIPTION OF STUDY -----	19
D. OPBL MODEL DATA ASSIMILATION -----	21
II. INSERTION OF SIMULATED TEMPERATURE PROFILES -----	23
A. INSERTION METHOD -----	23
B. WINTER REGIME -----	27
C. SPRING TRANSITION -----	34
D. SUMMER REGIME -----	41
E. NEW PROFILE INSERTION CONCLUSIONS -----	48
III. CREATION OF AND PREDICTION FROM SIMULATED TEMPERATURE DATA -----	52
A. SELECTION OF SEED PROFILES -----	52
B. ADDITION OF RANDOM ERRORS -----	53
C. ASSIMILATION OF SIMULATED TEMPERATURE OBSERVATIONS -----	56
D. FORECASTS BASED ON AVERAGES AND SCREENED AVERAGES -----	57
E. ERROR CALCULATIONS -----	59
IV. RESULTS OF FOURTEEN PREDICTION YEARS -----	61
A. RESULTS FROM INDIVIDUAL YEARS -----	61

1. Small Error Years -----	61
2. Positive Depth Error Bias Years -----	66
3. Negative Depth Error Bias Years -----	71
B. RESULTS BASED ON FOURTEEN YEARS -----	77
V. SUMMARY-----	85
A. CONCLUSIONS -----	85
B. RECOMMENDATIONS -----	87
APPENDIX A: SENSITIVITY OF THE GARWOOD OPBL MODEL TO VARIATIONS IN VERTICAL RESOLUTION -----	89
A. REASON FOR STUDY -----	89
B. EFFECT ON RUNS WITHOUT INSERTION -----	89
C. EFFECT ON INSERTION RUNS -----	96
APPENDIX B: RANDOM SELECTION OF SEED PROFILES -----	104
APPENDIX C: GENERATION OF RANDOM ERRORS IN TEMPERATURE AND DEPTH -----	106
BIBLIOGRAPHY -----	107
INITIAL DISTRIBUTION LIST -----	109

LIST OF TABLES

TABLE

1. Existing model temperature profile and replacement profiles for Julian Day 30, 1964 at OWS PAPA -----	29
2. Similar to Table 1, except for Julian Day 133 -----	36
3. Similar to Table 1, except for Julian Day 200 -----	43
4. Summary of insertion of erroneous temperature profiles into the model during three oceanic regimes at OWS PAPA in 1959 -----	49
5. RMS and bias errors (meters) for nine methods of forecasting mixed layer depth, based on 3-hourly predictions over a 15-day period at OWS PAPA in 1962 -----	64
6. Similar to Table 5, except for 1956 -----	69
7. Similar to Table 5, except for 1965 -----	74
8. Fourteen year ensemble of RMS and bias errors (meters) for nine methods of forecasting mixed layer depth, based on 3-hourly predictions over a 15-day period at OWS PAPA -----	83
9. Summary of the sensitivity of the Garwood OPBL model to variations in vertical resolution -----	103

LIST OF FIGURES

FIGURE

1.	Idealized temperature profile for the upper 200 m of the ocean -----	13
2.	Model-predicted maximum daily depths of the well-mixed layer (a), layer temperature minus 0.2°C (b), layer temperature minus 1.0°C (c), and layer temperature minus 2.5°C (d) at OWS PAPA during 1959 -----	18
3.	Linear approximations (L1 and L2) of the upper 200 m temperature profile (1964) on Day 30, 1964 at OWS PAPA -----	25
4.	Existing temperature profile (1964) and re- placement profiles for Julian Day 30, 1964 at OWS PAPA -----	28
5.	Model-predicted mixed layer depths for Julian Days 31-45, 1964 for control run (1964) and selected replacement profiles. Divisions on the time axis represent local noon at OWS PAPA --	30
6.	Model-predicted mixed layer temperatures for Julian Days 31-45, 1964 for control run (1964) and selected replacement profiles. Divisions on the time axis represent local noon at OWS PAPA -----	31
7.	Similar to Fig. 4, except for Julian Day 133 ----	35
8.	Similar to Fig. 5, except for Julian Days 134-148 -----	38
9.	Similar to Fig. 6, except for Julian Days 134-148 -----	39
10.	Similar to Fig. 4, except for Julian Day 200 ----	42
11.	Similar to Fig. 5, except for Julian Days 201-215 -----	45
12.	Similar to Fig. 6, except for Julian Days 201-215 -----	46

FIGURE

13. Addition of random errors to seed profiles to create simulated temperature profiles. Seed profile represented by thin line, arrows represent added temperature errors, heavy line represents simulated temperature profile ----- 55
14. Forecast paths for a winter regime study using five simulated temperature profiles. Forecasts based on the screened average of observations (a), the average of all observations (b), and on the last available profile only (c), and control run (d). Location of simulated temperature profiles represented by stars (e) ----- 58
15. Errors in forecasts of mixed layer depths for 1962 from predictions based on the last of 15 simulated profiles (a), the average of 15 simulated profiles (b), and the screened-average of 15 simulated profiles (c). Divisions on the time axis are 0000 GMT of Julian Day. Positive error represents layer depths forecast larger than the control run depth ----- 62
16. Errors in forecasts of mixed layer temperatures for 1962 from predictions based on the last of 15 simulated profiles (a), the average of 15 simulated profiles (b), and the screened-average of 15 simulated profiles (c). Divisions on the time axis are 0000 GMT of Julian Day. Positive error represents layer temperatures forecast larger than the control run temperature ----- 65
17. Similar to Fig. 15, except for 1956 ----- 67
18. Similar to Fig. 16, except for 1956 ----- 70
19. Similar to Fig. 15, except for 1965 ----- 73
20. Similar to Fig. 16, except for 1965 ----- 75
21. Model-predicted mixed layer depths for Julian Days 50-54 for control runs in 1958, 1961, 1965, and 1969. Divisions on the time axis represent 0000 GMT of Julian Day ----- 79
22. Root-mean-square errors in predicted layer depths for ensemble of 14 years based on the last of 30 simulated profiles (a), the average of 30 simulated profiles (b), and the screened-average of 30 simulated profiles (c). Time-axis divisions represent 0000 GMT on Julian Day ----- 81

FIGURE

23.	Similar to Fig. 22, except for mixed layer temperature errors -----	82
24.	Model-predicted mixed layer depths for Julian Days 31-45, 1964 at OWS PAPA. Model runs are represented with vertical resolutions of 1, 2.5, and 5 m. Time-axis divisions represent local noon at OWS PAPA -----	91
25.	Similar to Fig. 24, except for Julian Days 134-148 -----	92
26.	Similar to Fig. 24, except for Julian Days 201-215 -----	93
27.	Model-predicted mixed layer depths for DEEP profile insertions on Julian Days 31-45, 1964 at OWS PAPA. Model runs are represented with vertical resolutions of 1, 2.5, and 5 m. Time-axis divisions represent local noon at OWS PAPA ---	97
28.	Similar to Fig. 27, except for Julian Days 201-215 -----	99
29.	Model-predicted mixed layer temperatures for DEEP profile insertions on Julian Days 201-215, 1964 at OWS PAPA. Model runs are represented with vertical resolutions of 1, 2.5, and 5 m. Time-axis divisions represent local noon at OWS PAPA -----	101

ACKNOWLEDGMENTS

The author wishes to express sincere gratitude to Professor Russell L. Elsberry of the Naval Postgraduate School for his guidance and support throughout the research and preparation of this thesis.

Professor Bill Garwood provided the OPBL model, read the manuscript, and provided the solutions to many of the problems encountered in the research. David Adamec provided the numerical code for the heart of the Garwood model, while Pat Gallacher was a constant source of assistance in the writing and use of additional computer programs and in the understanding of the model. Mike McDermet provided helpful suggestions and support in completion of drawings and figures. Dr. Henry Fleming of the National Environmental Satellite Service graciously provided the computer code for creating random errors which were used in simulating temperature structure data. Numerical work was done at the W.R. Church Computer Center of the Naval Postgraduate School.

Finally, the author would like to thank his wife, Nancy, without whose support and sacrifices, this project would not have been possible.

I. INTRODUCTION

A. THE OCEANIC PLANETARY BOUNDARY LAYER

The upper layer of the ocean is characterized by a region in which the water temperature is nearly isothermal. In the oceanic planetary boundary layer (OPBL), mixing due to atmospheric winds and upward surface heat flux maintains a nearly homogeneous temperature and salinity profile. For this reason, the OPBL is often termed the mixed layer. Depending on the strength of atmospheric winds and on the direction of the surface heat flux, the depth of the mixed layer can be as shallow as a few cm or as deep as 200 m or more.

Figure 1 is a representation of an idealized temperature profile of the upper 200 m of the ocean. An isothermal layer of temperature T exists in the uppermost h meters. Below this, there is a temperature jump, ΔT , over a small vertical distance, Δh . In this study, Δh is assumed to be 1 m unless otherwise specified. Below $z = h + \Delta h$, the temperature is a function of depth, decreasing to T_{200} at $z = 200$ m.

Climatologically, the mixed layer is deep during the winter and shallow during the summer. The spring transition from deep to shallow layers is often very rapid [Budd, 1980], while the autumn transition to large layer depths through entrainment at the base of the layer is a more gradual process. On a synoptic time scale, however, mixed layer depths are highly variable. The large stress and heat flux during

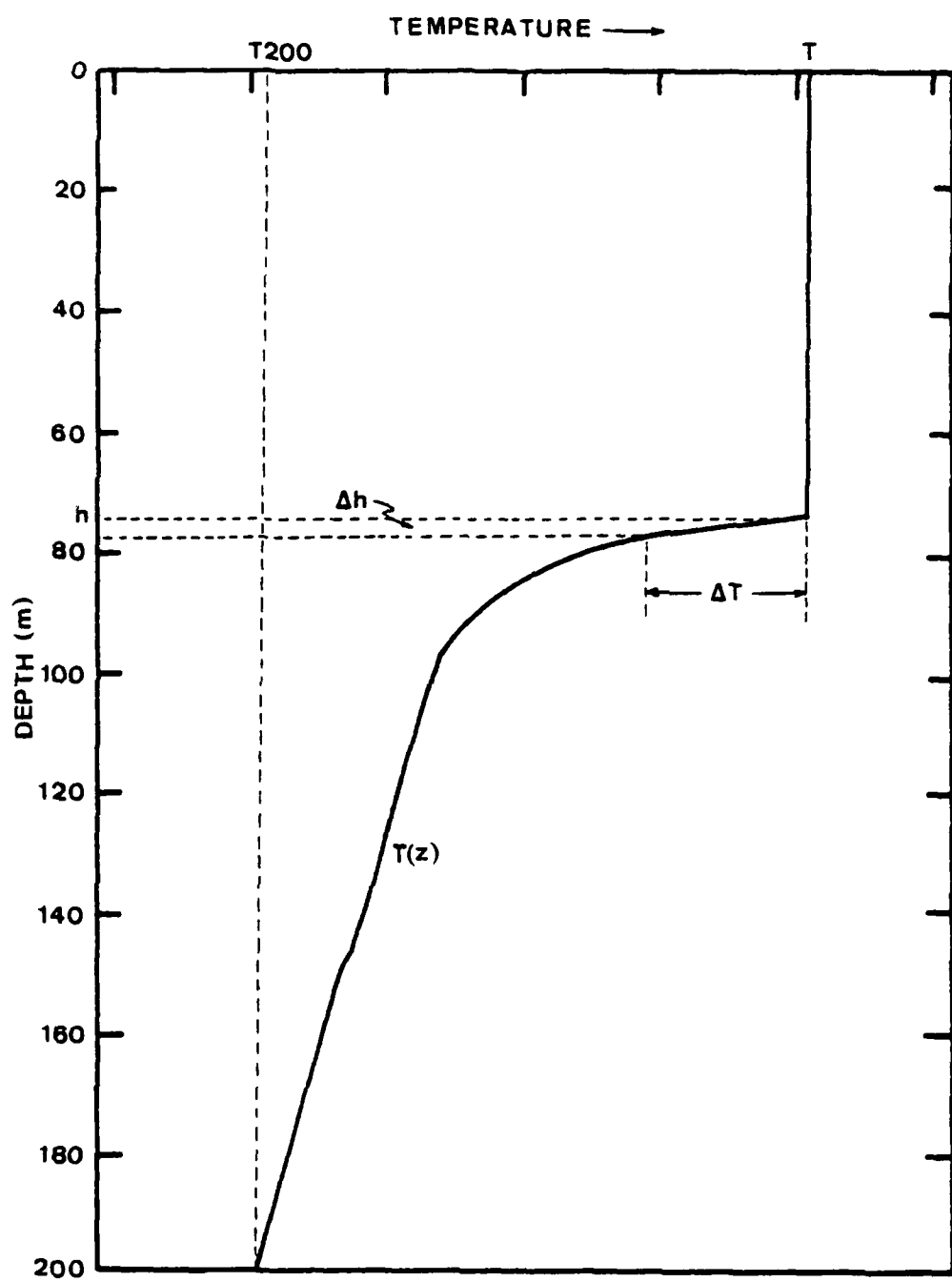


Fig. 1. Idealized temperature profile for the upper 200 m of the ocean.

atmospheric cyclones may quickly deepen and cool the oceanic mixed layer [Camp and Elsberry, 1978]. However, a period of weak winds accompanied by downward heat flux may cause the layer to shallow (retreat) to depths less than ten meters, even during the winter. An additional layer variability may occur with a diurnal cycle, deepening at night and retreating during daylight hours when downward heat flux at the surface is largest.

As the oceanic mixed layer changes through the year, periods of small mixed layer depths tend to be accompanied by increased layer temperatures, as the surface heating is confined to a small layer. Conversely, deep layers tend to be cold [Elsberry and Garwood, 1979]. Mixed layer depth varies more rapidly during the winter when the mixed layer temperature is nearly constant. During the summer the layer temperature varies greatly while the layer depth remains close to the mean value [Budd, 1980]. Layer temperature is naturally lowest during late winter and highest during late summer. A diurnal temperature cycle also exists, with highest temperatures during the afternoon and lowest during the hours before sunrise. The combination of layer temperature increase and layer depth decrease after local noon is known as the afternoon effect, which results in a warm, shallow layer whenever strong forcing by atmospheric winds is absent.

The ability to predict accurately mixed layer depths and temperatures would be beneficial in several areas. Temperature

profiles for the oceanic PBL in general, and mixed layer depths in particular, are essential to the U.S. Navy for anti-submarine warfare (ASW) operations utilizing sonar. Analyses based on local expendable bathythermograph (XBT) traces are helpful in sonar operation, but a reliable prediction of mixed layer thermal structure over a larger area would be invaluable to longer range planning and efficient use of surface ship, submarine, and aircraft assets. Fisheries management under the auspices of the National Marine Fisheries Service may also be aided by improved ocean thermal structure knowledge. A third area in which mixed layer forecasts may prove useful is in the understanding of long-range meteorological forecasting. For years, large scale climatology has been related to ocean surface temperature [Bjerknes, 1966 and 1972; Rowntree, 1972; and Namias, 1973 and 1976]. Improved knowledge of upper ocean heat structure and distribution may assist research in this area and improve long-range weather forecasting.

B. REQUIREMENTS FOR AN OPERATIONAL OPBL PREDICTION MODEL

Elsberry and Garwood [1979] pointed out similarities between numerical weather prediction and numerical ocean modeling. Numerical meteorology has proceeded at a faster pace than numerical oceanography. Present research in ocean prediction parallels earlier atmospheric work.

At present there are no oceanic mixed layer prediction models in operational use. One of the predictive models

being developed is the Garwood oceanic mixed layer model [Garwood, 1977]. This vertically integrated bulk model utilizes an entrainment hypothesis which is dependent on the relative size of horizontal and vertical components of turbulent energy. This mechanism is plausible in both entrainment and retreat cases. The model is distinguished by two important properties. The first is that the part of the wind-generated turbulent kinetic energy which increases potential energy by deepening the mixed layer is dependent on stability. This results in modulation of the entrainment rate by the diurnal heating/cooling cycle. The second property of interest is the Garwood model's ability to maintain a cyclical steady state over an annual period. This is accomplished by assuming a planetary influence on the dissipation time scale for turbulence, which enhances dissipation for deeper mixed layers.

Inputs are made to the model under the general heading of atmospheric forcing. The values for this study were taken from 3-hourly observations of wind speed, cloud cover, sea surface temperature, air temperature, and dew point, taken at ocean weather ship PAPA (50°N , 145°W). Three-hourly values of the forcing parameters were interpolated to one-hourly values. The hourly atmospheric forcing parameters were then used to calculate the time-dependent input values required for the Garwood model--the fluxes of buoyancy and momentum. Garwood defines buoyancy as the "reduced gravity"

effect caused by variation in heat and salt content. In this study the salinity profile is held constant. If salinity were allowed to vary during the run, hourly values of precipitation and evaporation would be required as part of the surface forcing.

Model outputs are the entrainment fluxes, mixed layer depth, mean temperature and salinity (buoyancy) in the layer [Gallacher and Garwood, 1980]. As the mixed layer depth retreats, heat, salt, buoyancy, and potential energy are conserved. When entrainment occurs, heat and salt are conserved and potential energy is increased.

Garwood and Adamec [1980] present a series of one-dimensional model runs using ship PAPA forcing. The model was started from an initial temperature profile observed at ship P on 1 January and run for 360 days. Figure 2 is a graphical representation of the predicted temperature structure for 1959. The daily depths at 1500 GMT (0500 local time at ship P) were plotted. At this time the mixed layer depth was expected to be the daily maximum. The simulated mixed layer depth followed expected patterns. The maximum depths were mostly in excess of 100 m until Day 100, when a rapid retreat occurred to maximum daily depths between 15 and 70 m. From Day 295, when the summer regime began to break down, the maximum layer depth gradually increased to the end of the experiment. Superimposed on this annual cycle was a synoptic-scale variability related to atmospheric forcing. Deepening

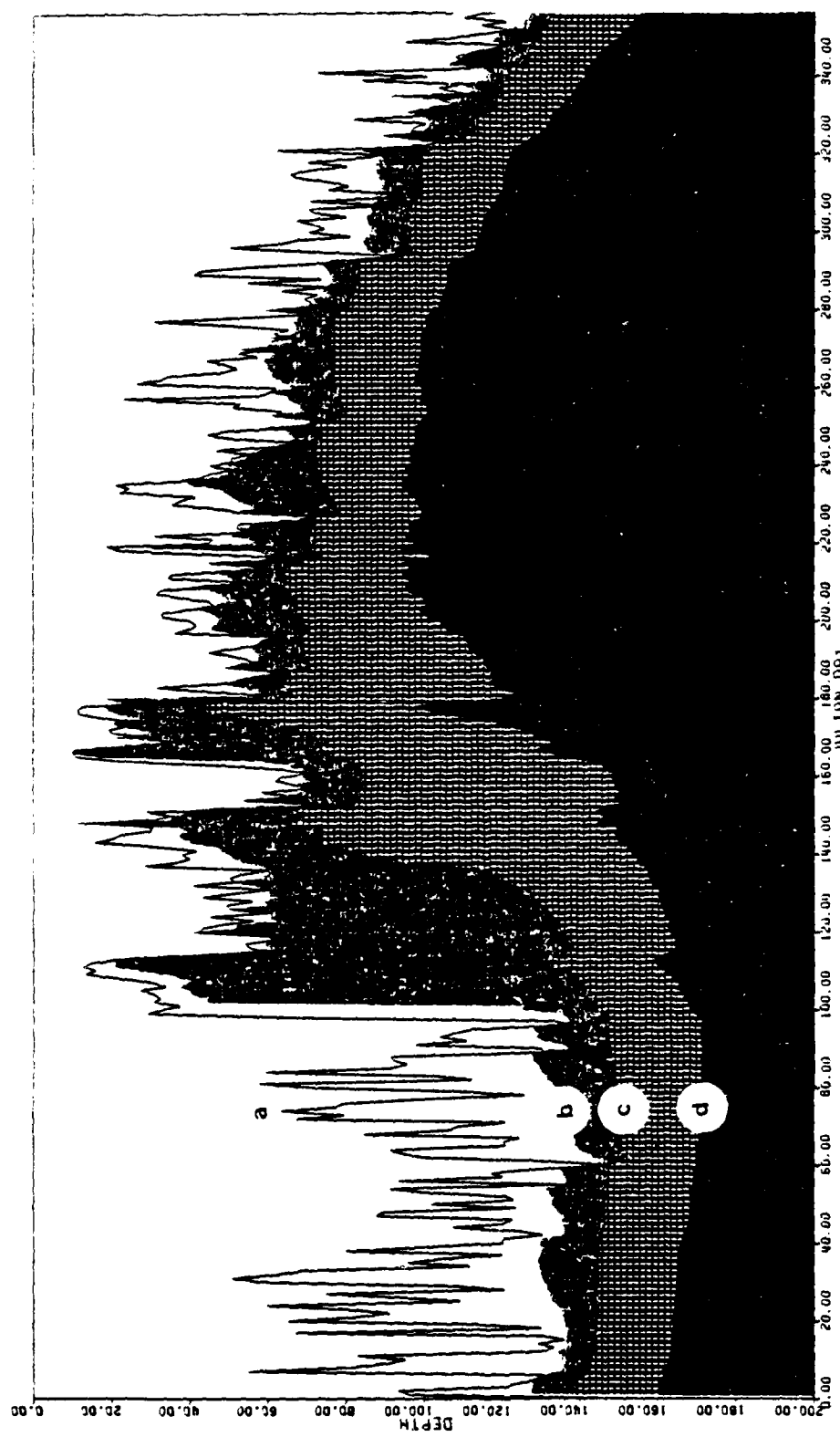


Fig. 2. Model-predicted maximum daily depths of the well-mixed layer (a), layer temperature minus 0.2°C (b), layer temperature minus 1.0°C (c), and layer temperature minus 2.5°C (d) at OWS PAPA during 1959.

events, associated with periods of strong turbulent mixing, occurred every three to four days, on the average. Observations of mixed layer depth at OWS PAPA in 1959 (not shown) exhibited the large scale trends and much of the short term variability of the Garwood-Adamec simulation.

C. DESCRIPTION OF STUDY

During the 360-day simulation, no corrections to the temperature profile were made. No thermal structure observations were necessary after the initial profile was used to start the model. However, ocean surface temperature observations were required to calculate the surface heat fluxes.

It was hypothesized that inclusion of more of the available temperature structure information would improve forecasts of oceanic mixed layer depths and temperatures. An experiment was devised to test this hypothesis. Observations are usually incorporated into numerical models during an analysis and initialization scheme which precedes the actual model integration. Data can also be inserted during the model run. This process, called data assimilation, was described for meteorological models by McPherson [1975]. In this study, data were inserted into the OPBL model before initialization and during the run. Development of an assimilation method to best use irregularly timed and spaced data observations is an important step in building an operational model.

The first step was to develop a method of including temperature structure information during a model run. This method of data assimilation had to be tested to insure that model outputs did not contain noise generated by the insertion procedure. The sensitivity to erroneous temperature profiles was first examined by assimilating various linear approximations of the model profile. Small or zero differences in layer depth and temperature predictions relative to the control run would indicate that the model assimilated the profile without generating damaging errors.

Tests were also made with the model using obviously erroneous profiles that were created for the winter and summer regimes, and for the spring transition. The profiles were based on the temperature structure which was to be replaced. Changes in layer temperature, layer depth, and the temperature jump at the base of the layer were added to test the reaction to various changes in temperature structure during the assimilation procedure.

Once the model's reaction to temperature structure changes during the run was determined, it was possible to create an experiment to test the main hypothesis. For this experiment, a number of temperature profile "observations" were simulated for a 15-day period in the model year. The winter regime (Days 35-50) was chosen. After the profiles were simulated, three predictions were made for the subsequent 15-day period (Days 50-64). The first prediction was made based on the simulated profile closest to Day 50. In

the second case, the simulated profiles were advanced to Day 50 using the model with the same atmospheric forcing as in the control run. These Day 50 profiles were averaged using time-weighting, and a prediction for Days 50-64 was made from the average profile. In the third case, any simulated profiles in which layer temperature or depth varied more than two standard deviations from the mean of the 15-day period were screened out prior to time averaging and prediction. If the hypothesis that increased use of temperature structure history improved forecasts was correct, the errors in predictions made from the average and screened-average of the simulated profiles should be smaller than the errors in the predictions based on the last profile alone.

Additionally, the amount of temperature history included in the test was varied. Five, fifteen, and thirty different profiles were simulated and used for averaging and prediction. Comparing errors in these predictions yielded information about how much temperature history should be used.

D. OPBL MODEL DATA ASSIMILATION

The long range objective of this research is to do an ocean simulation experiment similar to the atmospheric numerical simulations described by McPherson [1975]. He described a customary procedure for a simulation experiment in which a numerical prediction model was started from a certain initial state and integrated for several days. The model values extracted at specified times during this run were regarded as

"truth observations." The model was then integrated from an erroneous initial state and "observations" were periodically inserted. The degree to which the model state approached the control state was a measure of the extent of assimilation of the observations.

Initial oceanographic simulations revealed the property of "perfect assimilation" with the Garwood one-dimensional model. As defined by McPherson, the one-dimensional model immediately "forgets" previous profiles which existed before the observations were inserted. Thus, if a "true" observation were to be inserted, the model from that point on would make a forecast identical to the control run. For this reason, the oceanic numerical simulation had to be designed differently when the model in use was one-dimensional.

II. INSERTION OF SIMULATED TEMPERATURE PROFILES

A. INSERTION METHOD

It is plausible that inclusion of new temperature structure data during model runs would improve forecasts of mixed layer depth and temperature. The most complete temperature information comes from bathythermograph traces taken by surface (XBT), air (AXBT), or subsurface (SXBT) craft. Temperature is plotted as a function of depth from the surface to well below the base of the mixed layer. The temperatures are digitized and stored at specific depth intervals. Whether these stored temperatures can be used directly or must be interpolated depends on the vertical depth interval used in the model. The vertical sensitivity of the Garwood model is discussed in Appendix A. In this study, a vertical interval of 1 m was used.

Before using new temperature profiles derived from BT drops, it was necessary to study the sensitivity of the Garwood model to additional temperature information assimilated during the run. Data taken from ocean weather ship PAPA in 1964 were chosen arbitrarily as the subject of simulation experiments. The inserted profiles simulated conditions during the winter and summer, as well as during the spring layer retreat. These experiments demonstrate the sensitivity to insertions during different atmospheric forcing and oceanic thermal structure regimes.

The 1964 model run was halted and the existing temperature profile was replaced at 0000 GMT on Julian days 30, 133, and 200 at ship PAPA, stationed at 50°N, 145°W. The model was then restarted with the identical atmospheric forcing. Results from the new-profile runs were compared with results from the control run.

The insertion method was tested to insure that no unnecessary noise was introduced during the insertion and re-starting procedure. The model profile which existed on Day 30, 1964 at 2359 GMT is shown in Fig. 3. This profile was removed and replaced by two linear approximations (lines L1 and L2) in different runs. These approximations had the same mixed layer temperature, 4.89°C, layer depth, 114 m, and 200 m temperature, 2.80°C. L1 used a temperature jump in the meter below the layer of 0.81°C and L2 used a jump of 0.60°C.

Runs made by inserting profiles L1 and L2 at 0000 GMT on Day 31 yielded similar results. Both runs closely approximated the non-insertion results. Mixed layer temperatures remained within 0.02°C of the control values and the layer depths were within 1.8 m. It was concluded that the insertion method used to replace the temperature profiles provided viable results without introducing additional noise into the model.

The new temperature profiles inserted into the model during each period were intentionally created with large differences from the model-predicted profiles they replaced.

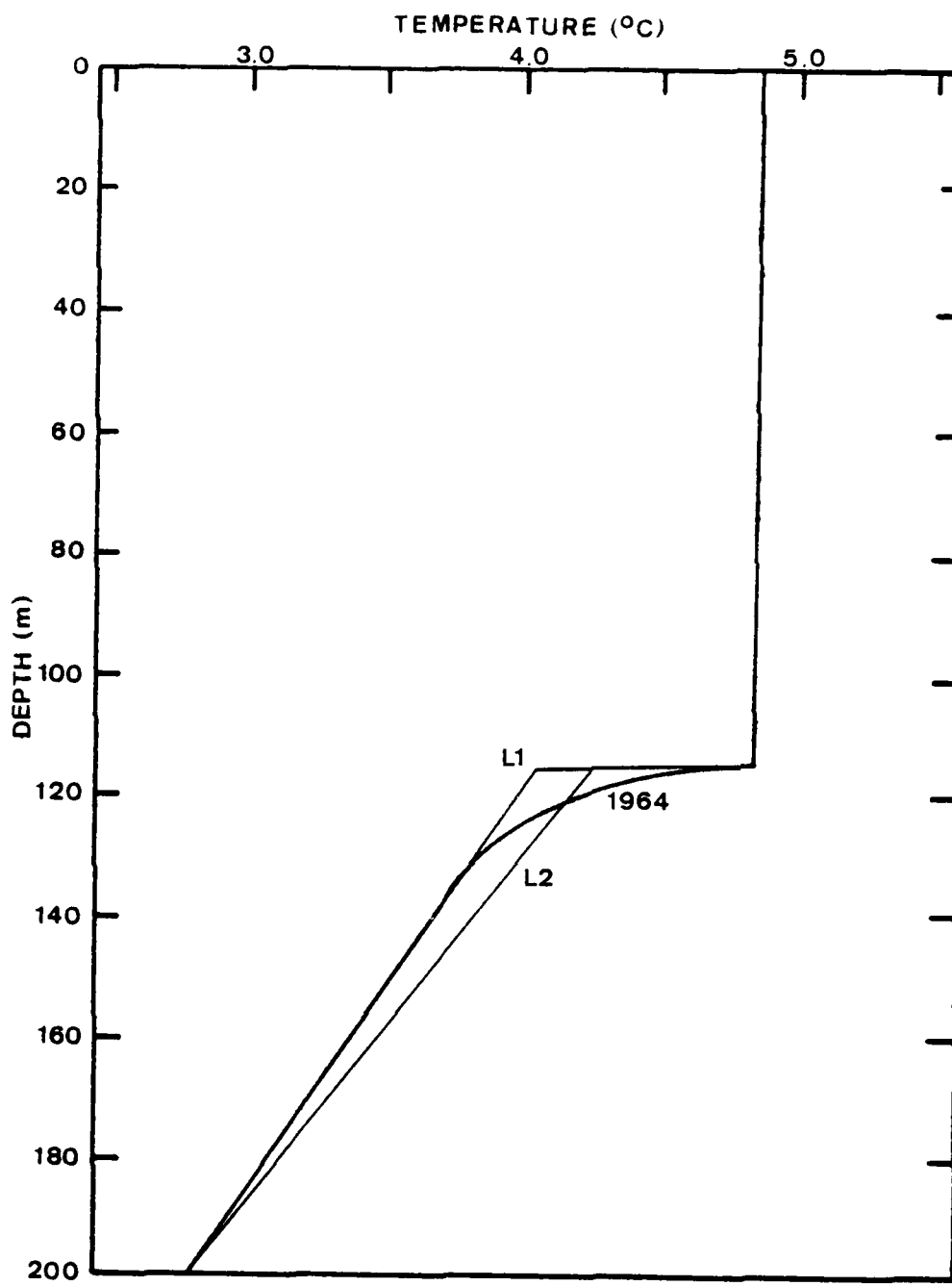


Fig. 3. Linear approximations (L1 and L2) of the upper 200 m temperature profile (1964) on Day 30, 1964 at OWS PAPA.

These differences can be considered to represent one of two real-world cases. The new values can be looked upon as correct observations inserted to update an incorrect model run. The differences can also be considered errors in observation of the temperature structure. Such errors could be caused by instrument errors in the BTs or recording equipment, errors in transcription or transmission, errors in data storage or retrieval, or by vertical distortion due to internal wave motion.

If the simulated values are thought of as exactly correct observations, the model absorbs them as desired, retaining the effect of the inserted values as the run continues. McPherson [1975] terms this "perfect assimilation."

If, on the other hand, the new values are considered to be erroneous observations, and the control data represent the correct values, the difference in the results represent errors in the model predictions. The relative size and persistence of the errors must be determined.

The simulated profiles were created by changing the mixed layer temperature or depth or the temperature jump at the base of the layer (h , T , or ΔT). The temperature below the layer decreased linearly from the value 1 m below the layer to 2.8°C at 200 m. This 200 m temperature was the initial condition in the 1964 data and remained unchanged throughout the 1964 model run.

Elsberry and Garwood [1979] point out that mixed layer depth and temperature respond directly to the frequency and

intensity of atmospheric forcing. Atmospheric forcing (wind, solar radiation, and surface heat flux) for the 1964 run was not altered when insertions were made in the model [Elsberry et al., 1979]. Thus, the insertion and control runs show strong correlation in every case.

Changes in the layer depth and temperature in the model caused by atmospheric forcing are made while conserving buoyancy and potential energy [Gallacher and Garwood, 1980]. Buoyancy represents the combination of temperature-induced and salinity-induced density effects [Garwood, 1977]. During these simulations the salinity profile was held constant with time, thus the conservation of buoyancy depended entirely on the conservation of heat.

B. WINTER REGIME

The five profiles which were inserted to replace the Day 30, 1964 profile are shown in Fig. 4 and Table 1. These erroneous profiles are designated WARM (higher T, same h, similar ΔT); DEEP (same T, deeper h, similar ΔT); SHALLOW (same T, smaller h, similar ΔT); LARGE (higher T, same h, larger ΔT); and SMALL (same T and h, smaller ΔT).

Mixed layer depths for the 15-day period following the insertion of the new profiles are displayed in Fig. 5. Corresponding mixed layer temperatures are shown in Fig. 6. Traces labeled 1964 represent the control run. Layer depths are highly variable, ranging from 5 to 120 m in the control run. Diurnal variations are obvious, especially between

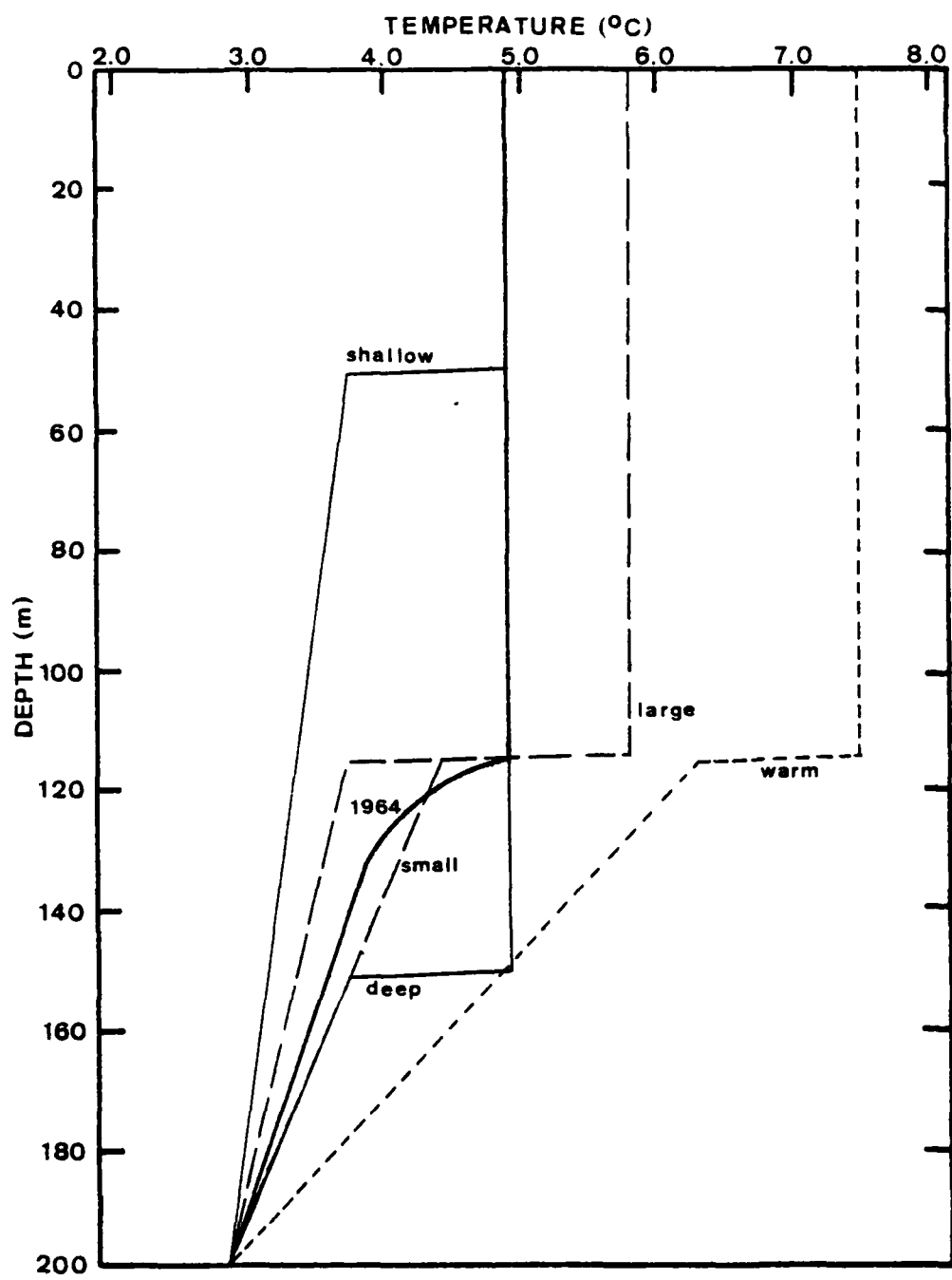


Fig. 4. Existing temperature profile (1964) and replacement profiles for Julian Day 30, 1964 at OWS PAPA.

Table 1

Existing model temperature profile and replacement
profiles for Julian Day 30, 1964 at OWS PAPA

<u>DESIGNATION</u>	<u>SURFACE TEMPERATURE, T (°C)</u>	<u>LAYER DEPTH, h(m)</u>	<u>TEMPERATURE JUMP, ΔT (°C)</u>
1964 Day 30	4.89	114	1.02/14 m
WARM	7.50	114	1.2
DEEP	4.89	150	1.2
SHALLOW	4.89	50	1.2
LARGE	5.80	114	2.1
SMALL	4.89	114	0.5

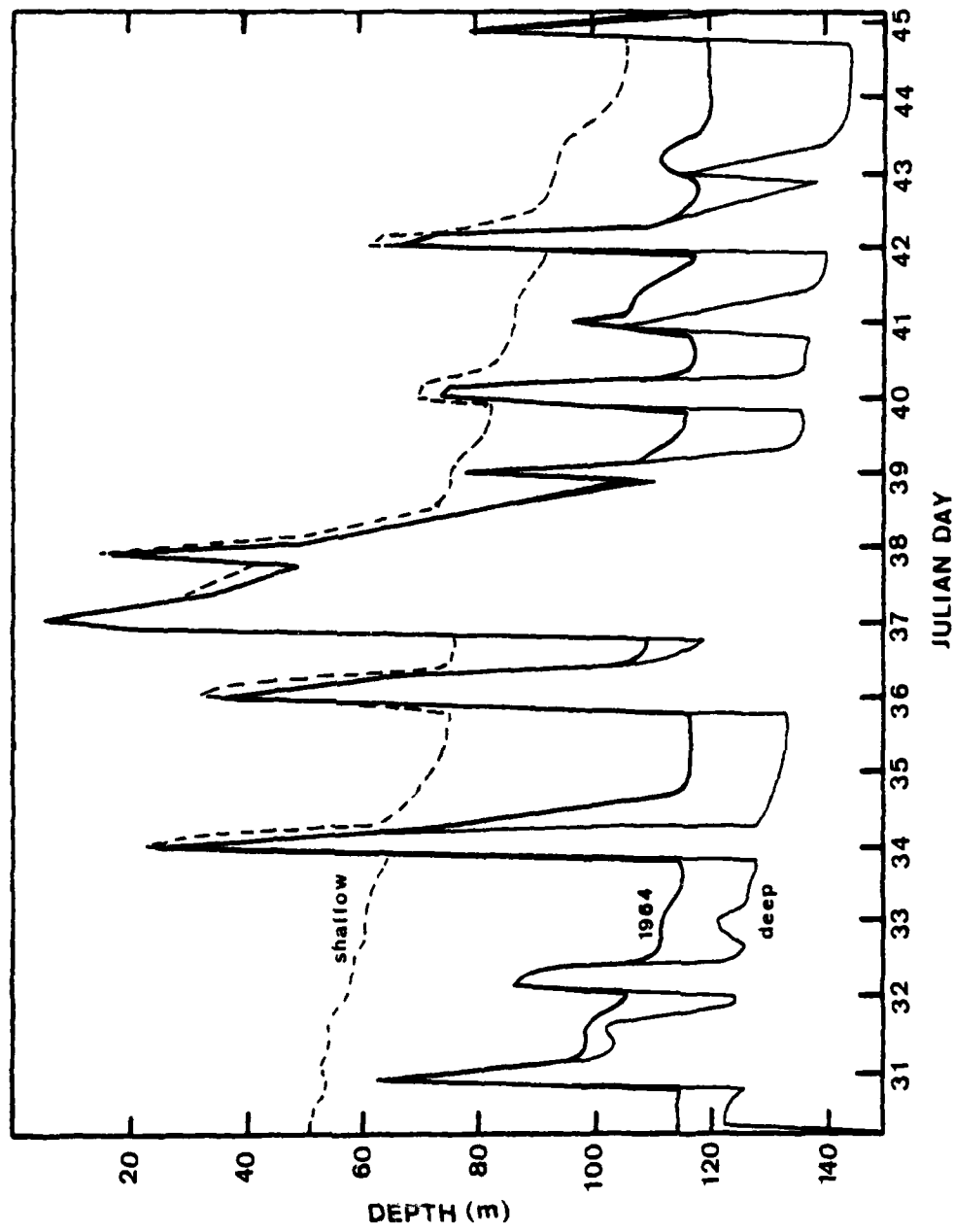


Fig. 5. Model-predicted mixed layer depths for Julian Days 31-45, 1964 for control run (1964) and selected replacement profiles. Divisions on the time axis represent local noon at OWS PAPA.

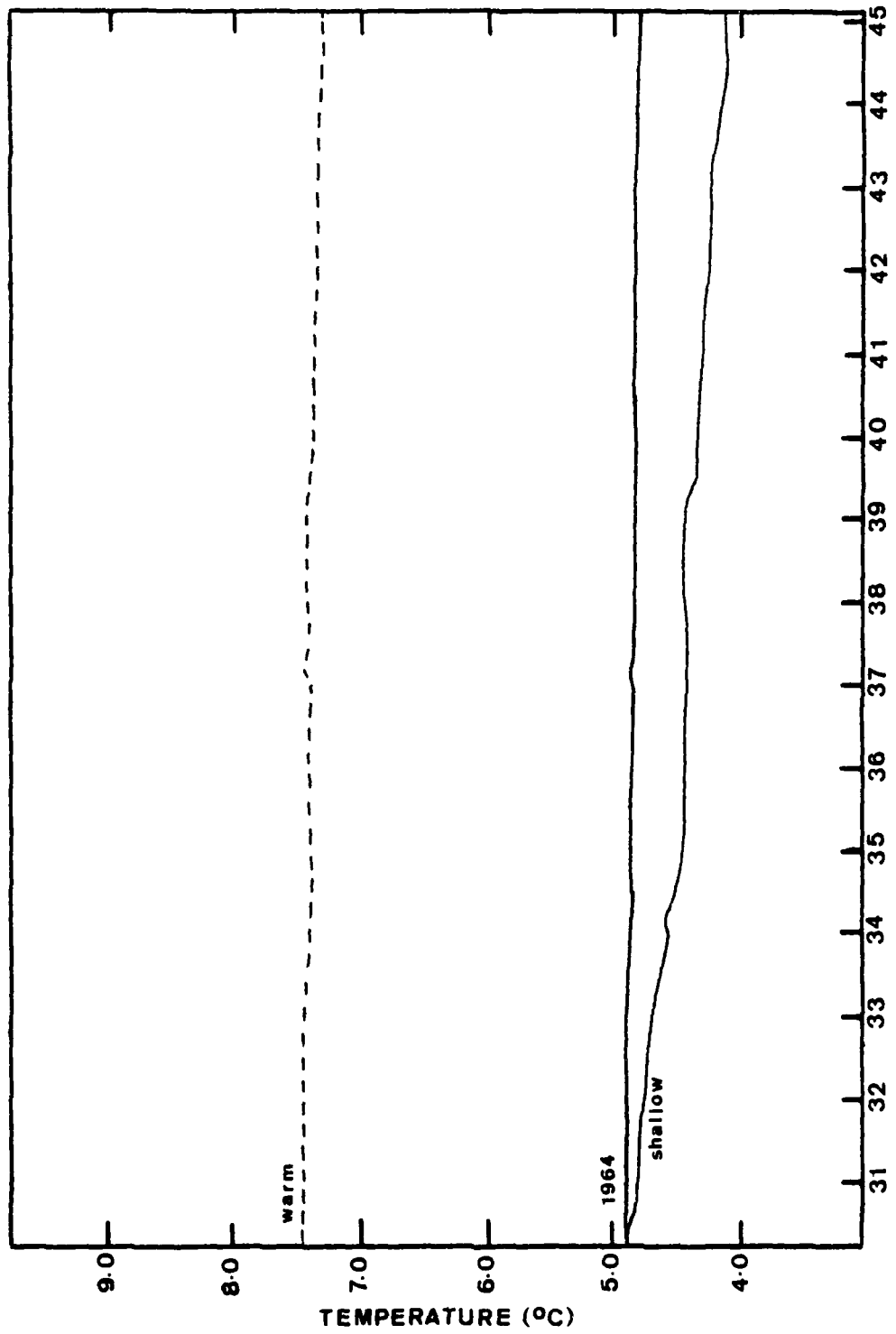


Fig. 6. Model predicted mixed layer temperatures for Julian Days 31-45, 1964 for control run (1964) and selected replacement profiles. Divisions on the time axis represent local noon at OWS PAPA.

Days 36 and 44, when noontime shallowing episodes occurred daily. The divisions along the time axes in the figures represent local noon at ship PAPA.

Mixed layer temperatures for the winter regime are nearly constant with respect to time. As the layer deepens and shallows over a wide range, the temperature varies little. Between Days 30 and 45 the layer cooled slightly ($\sim 0.15^{\circ}\text{C}$) in the control run.

Layer depths predicted by the model after the five replacement profiles were inserted followed similar diurnal patterns. The SHALLOW simulation replaced the model's layer depth (114 m) with $h = 50$ m. The layer temperature was maintained, resulting in less heat, and consequently, less buoyancy in the upper 200 m. The profile in the SHALLOW case was colder than the profile it replaced at all depths greater than 50 m. The potential energy of the SHALLOW mixed layer was smaller than the 1964 potential energy, since there was less warm water at depth. Conservation of the reduced buoyancy and potential energy resulted in the SHALLOW case mixed layer depths for Days 30-45 (Fig. 5). The layer depths gradually increased to within 15 m of the non-insertion value at the end of the 15-day period. When daily retreat phases caused shallowing to within 75 m of the surface, the depth in the SHALLOW simulation was within 3 m of the control depth. As the forcing increased the layer depth from 50 to 105 m, conservation of buoyancy required the layer temperature to

decrease. As is shown in Fig. 6, the temperature in the SHALLOW simulation decreased 0.8°C in 15 days.

The DEEP simulation began with a layer depth of 150 m and a profile that was warmer than the existing profile between 115 and 150 m. Within 3 hours the layer retreated to 122 m, indicating that the surface forcing was insufficient to maintain the erroneously large depth. The increased buoyancy and potential energy resulted in a small jump at the base of the layer and a nearly isothermal layer to 150 m. Throughout the 15-day period, the DEEP simulation layer depths exhibited the same pattern of diurnal variation as the control run. During retreat periods the DEEP layer depth coincided with the 1964 values. However, during the deepening periods between retreats, the marginal stability between 115 and 150 m allows the DEEP values to reach depths 15-25 m greater than the control. Unlike the SHALLOW case, the depths in the DEEP simulation paralleled the control case throughout the period. Consequently, the DEEP mixed layer temperatures remained the same as the 1964 temperatures throughout the run.

The mixed layer depth evolution was very similar to the control for all cases in which h was retained and the temperature or temperature jump was varied (WARM, LARGE, and SMALL). In all three cases the values remained within 11 m of the control values. Retreat and deepening periods showed strong correlation ($r = .985$ for SMALL). This indicates that a bias in temperature observation, or a real shift in T due

to horizontal advection, has little effect on the mixed layer depth during the winter. This result may be model dependent since the maximum potential MLD depends strongly on surface forcing.

Making the layer temperature higher at Day 30 did cause a persistent difference in layer temperature. In the WARM simulation the layer remained 2.61°C warmer from insertion through Day 45. Similarly, layer temperature in the LARGE profile was 0.91°C warmer upon insertion and 0.87°C warmer at the end of the period. The Garwood model completely "forgets" the previous profile upon assimilation of a new one. No adjustment, comparison, or blending takes place. Since heat flux is not dependent on the model sea surface temperatures, and the mixed layer depth was unchanged, the T evolution parallels the control run.

As was the case for the layer depths, the layer temperatures for all Day 30 runs were strongly correlated ($r = .920$ to $.986$). In the DEEP and SMALL simulations, which started at the same temperature as the control run, the temperatures remained within 0.05°C throughout the period.

C. SPRING TRANSITION

The purpose of this case was to determine model sensitivity to erroneous insertions during the spring layer retreat phase. The existing profile from Day 133 (12 May) 1964 and the replacement profiles which were inserted are shown in Fig. 7 and Table 2. Note that the temperature gradient below the

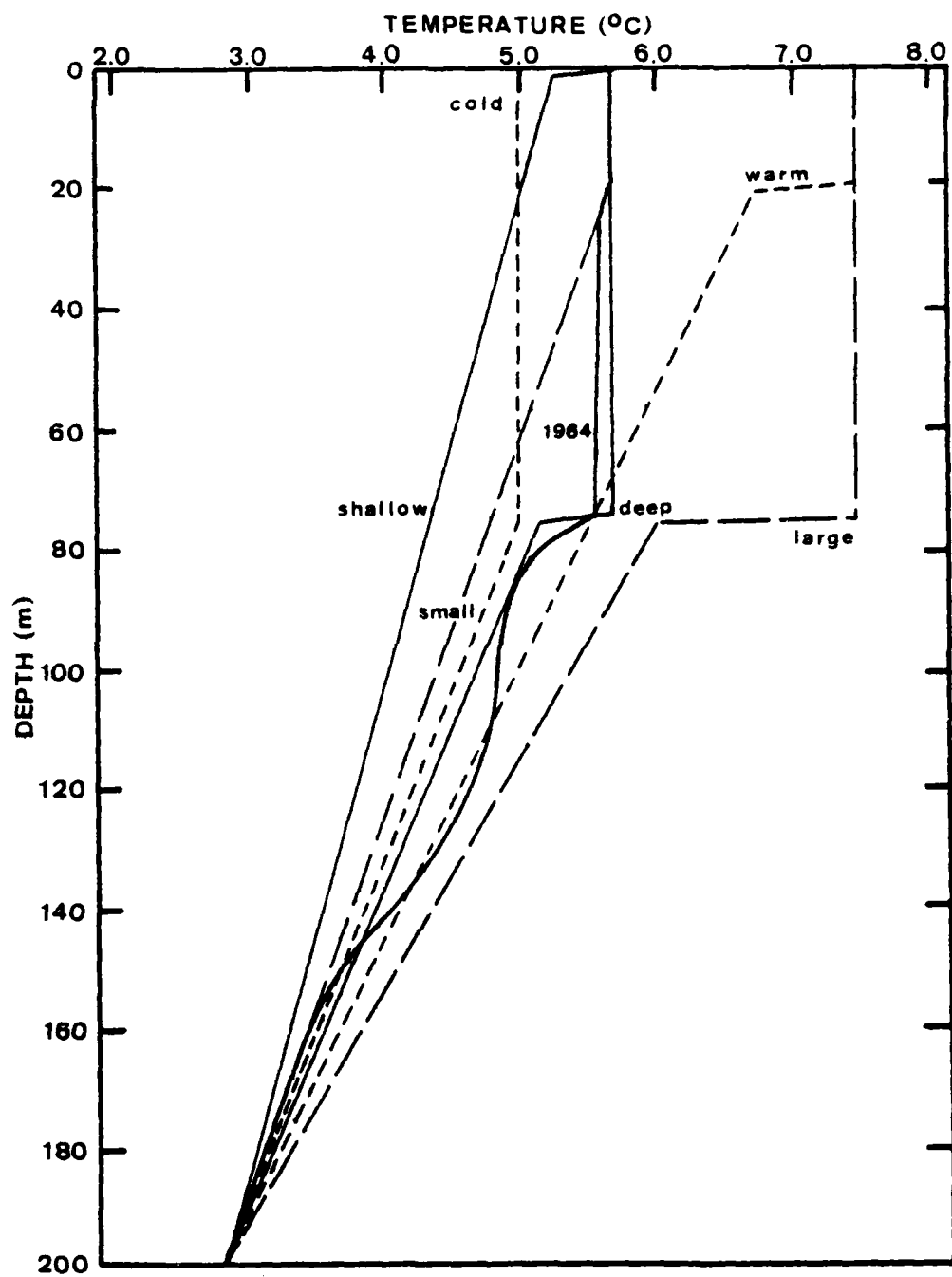


Fig. 7. Similar to Fig. 4, except for Julian Day 133.

Table 2
Similar to Table 1, except for Julian Day 133

<u>DESIGNATION</u>	<u>SURFACE TEMPERATURE, T (°C)</u>	<u>LAYER DEPTH, h (m)</u>	<u>TEMPERATURE JUMP, ΔT (°C)</u>
1964 Day 133	5.67	20	0.1/10 m
WARM	7.50	20	0.75
COLD	5.00	75	0.0
DEEP	5.67	75	0.53
SHALLOW	5.67	1	0.4
LARGE	7.50	75	1.5
SMALL	5.67	20	0.0

model-designated mixed layer depth (20 m) is only 0.06°C in 5 m. However, a more pronounced thermocline existed at 75 m with a temperature gradient at 0.4°C in 5 m. For this reason, three of the six replacement profiles, DEEP, COLD, and LARGE, were inserted with layer depths of 75 m. The DEEP profile was of special interest, since it closely approximated the profile which existed in the model just prior to insertion.

Mixed layer depths for Days 133-148 are shown in Fig. 8 and layer temperatures are shown in Fig. 9. The layer depth shows diurnal variability, as was the case in winter. On 14 of the 15 days the layer retreated around local noon. Layer depth varied from 41 m on Day 142 to 1 m (minimum h recognized by the model) on several occasions.

Layer temperatures showed a gradual warming trend during the period. Diurnal influences were obvious, with local temperature maxima occurring around 1700 local time each day. The large afternoon temperature increases on Days 134, 136, 147, and 148 corresponded to the days when the simulated layer depth decreased to 1 m during the afternoon.

The profile designated SHALLOW, which had an initial layer depth of 1 m, was colder than the control profile throughout the upper 200 m. The layer deepened to 20 m before retreating as in the control run on the afternoon of Day 134. During the deepening episode on Day 135, the layer depth remained within 7 m of the control until the afternoon of Day 136, and then was nearly identical to the control for

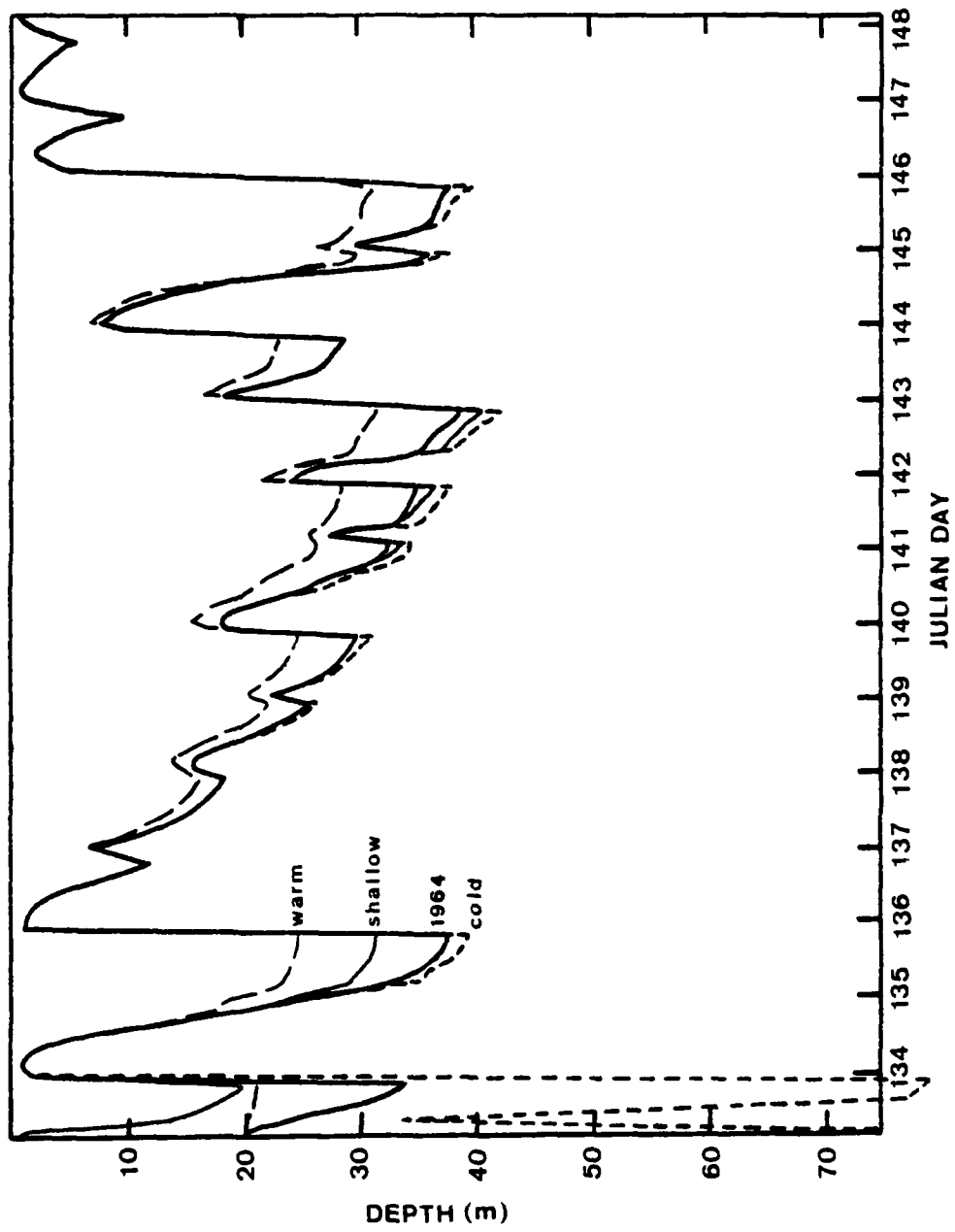


Fig. 8. Similar to Fig. 5, except for Julian Days 134-148.

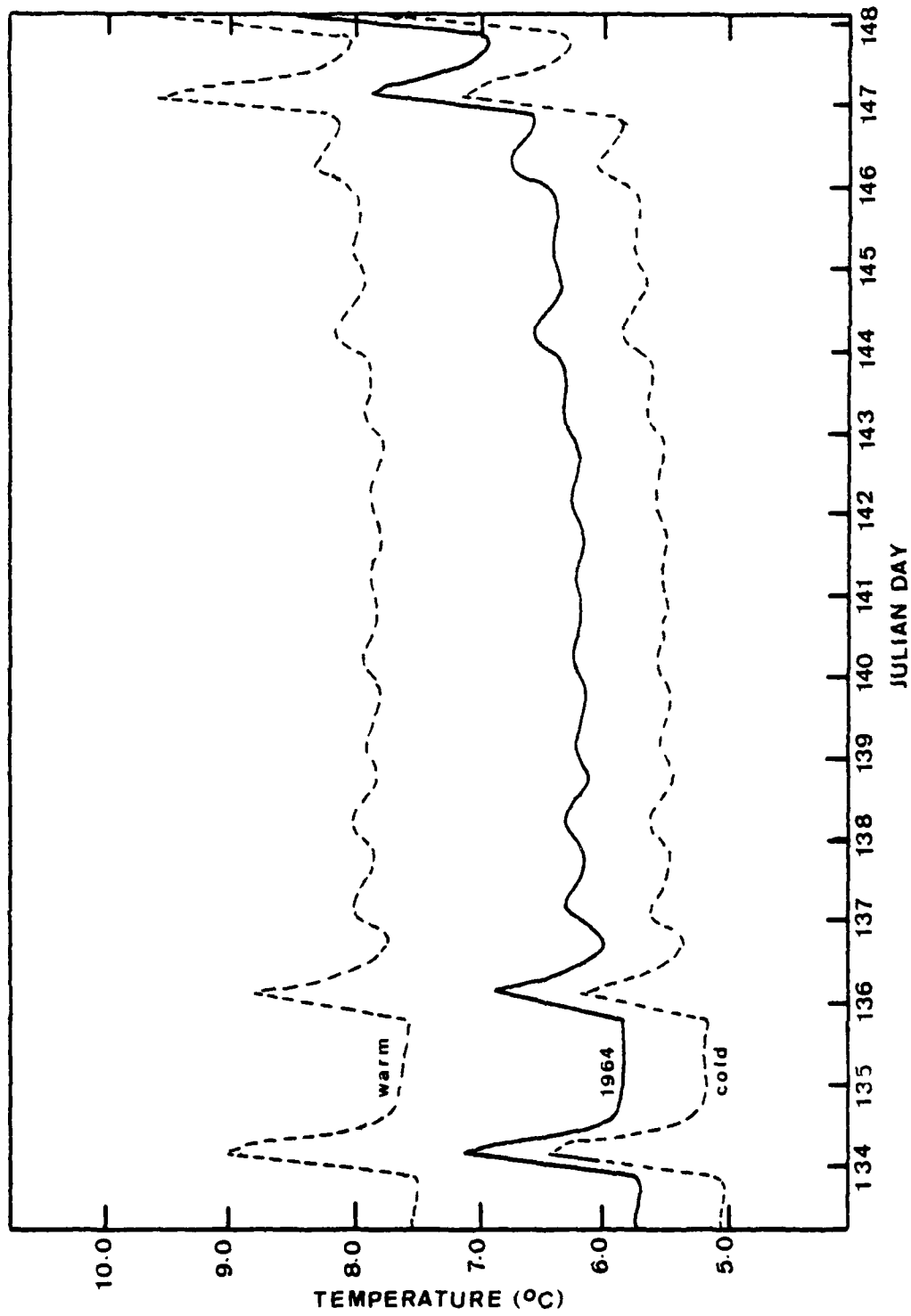


Fig. 9. Similar to Fig. 6, except for Julian Days 134-148.

the remainder of the period. The SHALLOW case started with a layer temperature equal to the control run ($T = 5.67^{\circ}\text{C}$). As in the winter regime, the conservation of the reduced buoyancy in the SHALLOW profile mandated a cooling trend as the layer deepened. As expected, the layer cooled 0.5°C in the first 18 hours and remained $0.5 - 0.6^{\circ}\text{C}$ colder throughout the period.

The DEEP profile simulation which was expected to closely approximate the control run, started with the same T but a layer depth of 75 m. As the surface forcing was not sufficient to maintain the excessive depth, the layer shallowed to 25 m in the first 3 hours after insertion. The DEEP profile matched the control run from 15 hours past insertion until the end of the period. Throughout the 15 days the layer temperature remained within 0.1°C of the 1964 value. As expected, correlation was nearly perfect ($r = .999$).

Greater variation from the control depth evolution was found in runs in which WARM and COLD profiles were inserted. The WARM profile, which had a large temperature jump at the base of the layer, was much more stable than the control. It was warmer through the top 75 m, and much warmer in the top 20 m. Consequently, the mixed layer depth remained consistently shallower than the control depth, being as much as 13 m shallower on Day 136.

In both the COLD and DEEP profiles, the initial layer depth was 75 m. However, the temperature jump in the COLD

simulation was much smaller than in the DEEP case. With the small stability at the base of the layer, the depth in the COLD run increased rapidly to 89 m on the morning of Day 134. However, this depth could not be maintained by the surface forcing, and the COLD mixed layer depth closely resembled the control following Day 135. The depths in the COLD case, while still well correlated with the 1964 data ($r = .886$), had the lowest correlation of the Day 133 insertions.

As was the case in the winter regime, layer temperature errors inserted at Day 133 remain in the model throughout the run. This bias is partly the result of heat flux calculations which are independent of the inserted sea surface temperatures.

D. SUMMER REGIME

The third period of interest was the summer regime, which may be characterized by a warm, shallow mixed layer and a strong seasonal thermocline. Test insertions were made on Day 200 (18 July) of 1964. The model profile at that time and the six replacement profiles are shown in Fig. 10 and Table 3.

Replacement profiles were created in the same manner as for Days 30 and 133. The three-part profiles--isothermal layer, 1 m temperature jump, and linear decrease bracketed the existing profiles on Days 30 and 133 (Figs. 4 and 7). However, the strong seasonal thermocline between 10 and 50 m

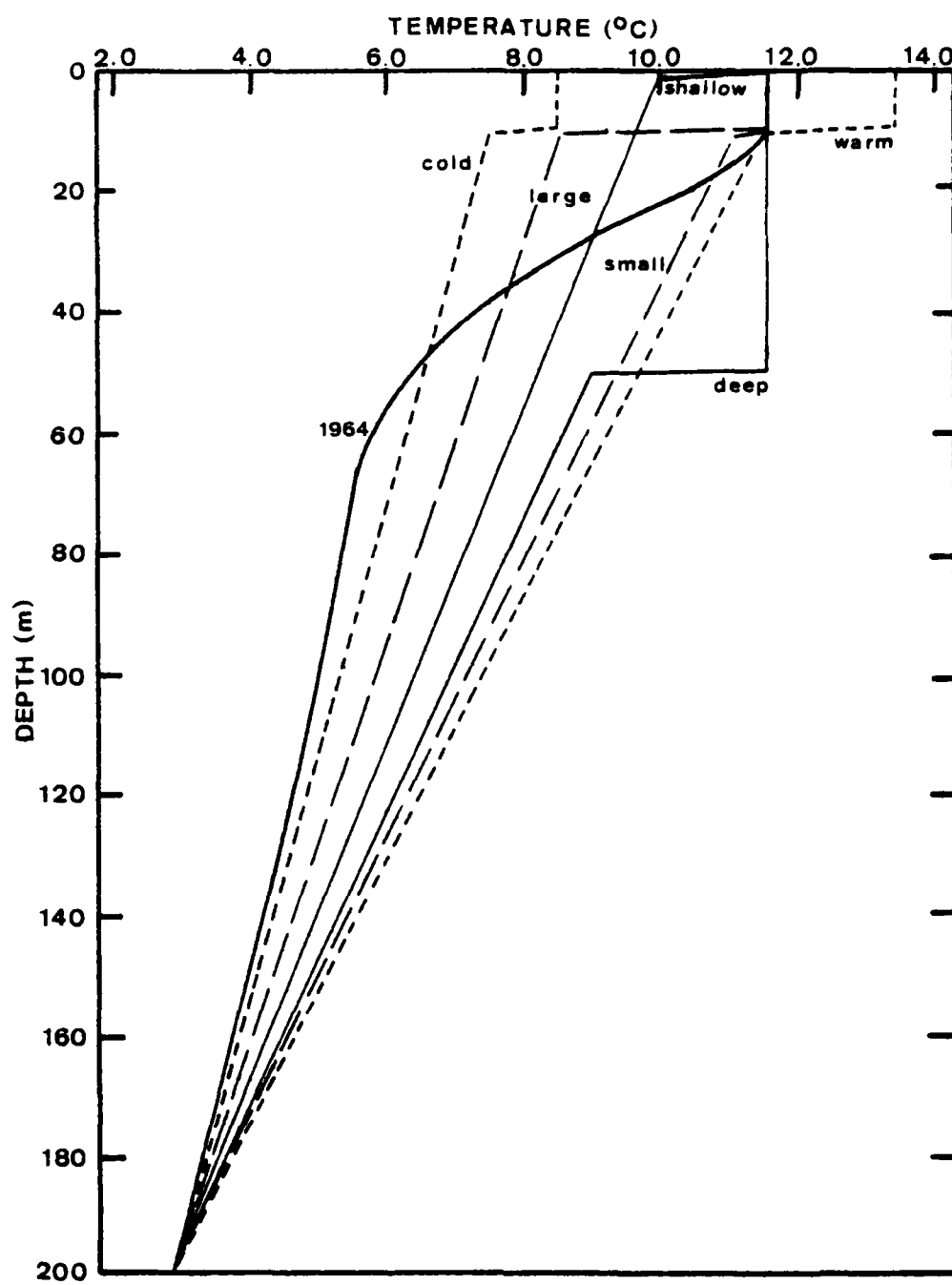


Fig. 10. Similar to Fig. 4, except for Julian Day 200.

Table 3
Similar to Table 1, except for Julian Day 200

<u>DESIGNATION</u>	<u>SURFACE TEMPERATURE, T (°C)</u>	<u>LAYER DEPTH, h (m)</u>	<u>TEMPERATURE JUMP, ΔT (°C)</u>
1964 Day 200	11.58	10	1.1/10 m
WARM	13.50	10	2.10
COLD	8.50	10	1.00
DEEP	11.58	50	2.58
SHALLOW	11.58	1	1.58
LARGE	11.58	10	3.00
SMALL	11.58	10	0.50

made the model profile colder than all replacement profiles below 45 m. The Day 200 insertions tested the effect of this temperature excess below the mixed layer.

Mixed layer depths for the Day 200 simulations are shown in Fig. 11. The control run resulted in depths ranging between 1 and 24 m. Afternoon retreats to layer depths of 1 to 15 m occurred on 10 of 15 days. Layer temperatures are shown for several assimilation runs in Fig. 12. The overall trend of the 1964 run was a slight warming of the layer over the fifteen days. Diurnal effects are evident with maximum temperatures around 1700 local time daily. Rapid warming on Day 202 (1.4°C) corresponded to rapid layer retreat to 1 m on that afternoon.

The DEEP profile ($h = 50$ m) and the SHALLOW profile ($h = 1$ m) were inserted and showed a similar depth evolution after a short period of adjustment. In the DEEP case the layer depth retreated to less than the control run value within 3 hours after insertion. The SHALLOW run layer depth increased to the control value by local noon on Day 201. From Day 201 to Day 215 the layer depths in both the DEEP and SHALLOW simulations nearly coincided with the control run, reaching a maximum of 27 m on the morning of Day 212 (3 m deeper than the contr-1). Both insertions showed high correlations ($r = .981$ for SHALLOW and $.985$ for DEEP).

It is apparent that the added buoyancy at depths greater than 20-25 m had little effect on the layer depth as predicted

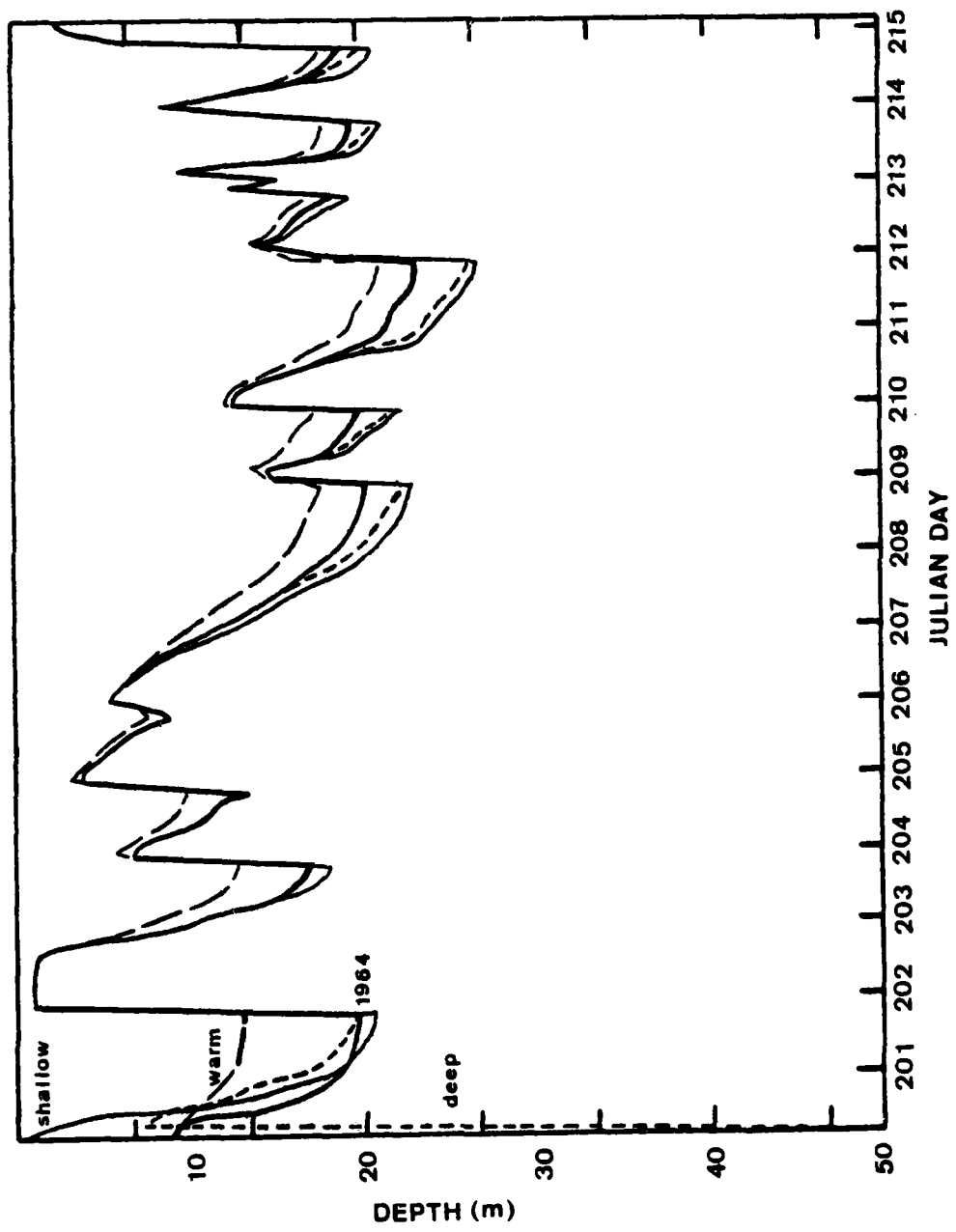


Fig. 11. Similar to Fig. 5, except for Julian Days 201-215.

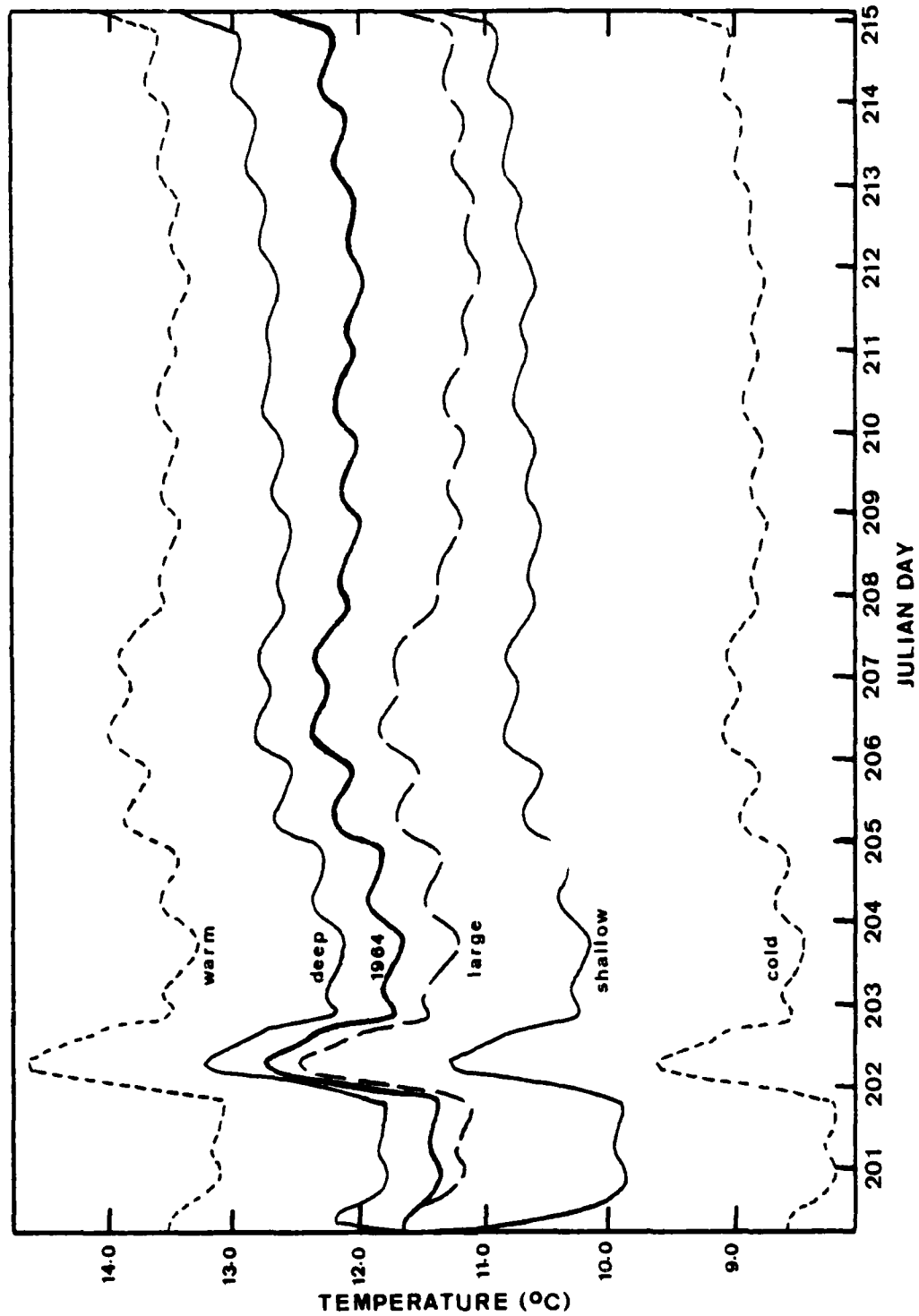


Fig. 12. Similar to Fig. 6, except for Julian Days 201-215.

by the model. The effect of the deeper water was not felt because strong downward buoyancy flux at the surface (which increases stability), combined with weak mechanical mixing, could maintain a layer depth of only 25 m or less.

Layer depths in the WARM and LARGE cases were consistently smaller than the non-insertion run, with differences as much as 5 m during the deepest parts of the diurnal cycle. Both of these profiles had warm layers in the upper 10 m with a large ΔT at the base. The result of this concentration of buoyancy near the surface is a very stable profile. The available energy for mixing had less effect on these stable profiles than on the less stable control profile.

Unlike the summer regime layer depths, which differed little from the control values, the mixed layer temperatures diverged greatly. In addition to initial biases in the WARM and COLD simulations, insertions of profiles with the initial T equal to the control (DEEP, SHALLOW, and LARGE) also resulted in large variations in layer temperature (Fig. 12).

It is interesting to note the effect of changing the layer depth on the resulting layer temperatures. Immediately after insertion, the layer temperature increased/decreased in the DEEP/SHALLOW simulations, becoming 2°C different 18 hours after insertion. This difference was maintained throughout the 15-day period. As the model adjusted the erroneous layer depths, it conserved buoyancy and potential energy. The buoyancy deficiency of the SHALLOW profile between the surface and 25 m resulted in a lower layer

temperature. Conversely, the buoyancy excess below 10 m in the DEEP case caused the temperature to rise as the layer retreated.

The WARM profile run started with a surface temperature 1.92°C higher than the control value. Diurnal variations were similar, but the difference decreased to 1.4°C by Day 215. Similarly, the layer temperature in the LARGE simulation cooled 1°C with respect to the control. Downward flux of buoyancy at the surface caused the control layer to warm slightly during the run. This warming trend was negated in the WARM and LARGE cases, in which stable layers were mixed with much colder water below.

The SMALL ΔT profile was warmer than all other profiles (excepting WARM) below 50 m. Insertion resulted in layer depths within 2 m and temperatures within 0.1°C throughout the period. Effects of the increased buoyancy and potential energy below 50 m appear to be negligible during the summer regime.

E. NEW PROFILE INSERTION CONCLUSIONS

The conclusions drawn from this phase of the study are summarized in Table 4. In all cases, the mixed layer depth followed the shallowing and deepening pattern dictated by the atmospheric forcing. During retreat episodes, when forcing was not sufficient to maintain existing depths, the values present in all simulation runs closely matched the control value. Periods of deepening revealed that observation

Table 4

Summary of insertion of erroneous temperature profiles into the model during three oceanic regimes at OWS PAPA in 1959

<u>Changes inserted</u>	<u>Shallowing</u>	<u>Deepening</u>
Initial MLD > control	When forcing is insufficient to maintain greater depth, the value coincides with the control.	Will tend to reach deeper depths due to lower stability below the initial MLD of the control.
Initial MLD < control	Depth returns to the control value.	Deepening impeded, resulting in shallower layer. Conservation of buoyancy causes layer to cool.
Initial ΔT large	Little effect.	Stability impedes deepening, resulting in shallower layer. Layer cools due to conservation of buoyancy, especially in summer.
Initial ΔT small	Little effect.	Decreased stability at the base of the layer allows more rapid deepening and slightly larger maximum depths.
Initial ΔT > control	Parallels control T but retains high (low) bias.	Parallels control T while retaining high (low) bias. High T increases stability and impedes deepening. Lower T allows increased deepening.

errors affect deepening rates and maximum depths. In winter especially, when the surface buoyancy flux is upward and mechanical mixing is strong, mixed layer depths show large variations.

Errors in the observed layer depth have relatively large effects in the resulting layer temperature predictions, especially in the summer, when the layer is shallow. If too shallow a layer is inserted, it will soon deepen to nearly the correct depth. However, conservation of buoyancy requires that this deepening be accompanied by cooling as the warm water in the layer mixes with cooler water below. In all simulations, insertion of a shallow layer at the correct temperature soon resulted in a layer temperature which was too cold. Insertion of a deep mixed layer in the summer case resulted in too warm a layer when the layer depth retreated.

Errors in temperature observations result in mixed layers which remain too warm or too cold. In no case did the temperature of the layer show a tendency to return to the "correct" value. Temperature errors also affect subsequent deepening of the layer, especially if the observed temperature is too warm. In these cases, the increased buoyancy in the upper layers and more stable water columns induced shallower layer depths.

Changing the size of the temperature jump at the bottom of the layer had comparatively smaller effects on the resulting layer temperature and depth predictions. A large ΔT made the

layer more stable and resulted in smaller layer depths during the deep phases of the cycle. Insertion of a small jump (or no jump) at the bottom of the layer reduces stability, allowing deepening to greater depths. This effect was not significant in SMALL tests, but is evident in the Day 133 COLD simulation. In this case a deep, cold layer with no jump at the base was sufficient to allow deepening to 84 m when the control depth was only 33 m.

The summer case had a water column colder than the simulation profiles at all depths below 45 m. The results of the Day 200 insertions showed the changes in layer temperature were more sensitive to temperature differences in the layer than below it. For example, the SHALLOW profile was initially colder between 1 and 27 m, but was warmer from 27 to 200 m. Resulting layer temperatures were approximately 1.5°C colder throughout the run.

III. CREATION OF AND PREDICTION FROM SIMULATED TEMPERATURE DATA

A. SELECTION OF SEED PROFILES

After testing the erroneous data insertion effects with the Garwood model, it was possible to design a numerical simulation to test the main hypothesis of the study. The hypothesis was that using available temperature history to initialize the mixed layer model would improve forecasts over initialization from the most recently observed profile.

Use of observed temperature profiles from OWS PAPA (or elsewhere) would have introduced the possibility of data contamination from any of several sources. Changes in sensing or recording equipment, changes in personnel, or influences of advection processes could have caused biases in the data which could not have been identified or controlled in the experiment. In addition, the only way to vary the number of profiles to be considered in the data insertion would have been to delete some of the observed profiles. This is not desirable because there are generally too few observations available. To avoid these problems, it was decided to use model-generated data whose frequency and accuracy could be controlled.

The period for which the simulated profiles were created was the fifteen days prior to the beginning of the forecast. In this study the "forecast window" was from Julian Day 50

to Day 64 and the "history window" was Days 35 to 49. The simulated profiles were created from seed profiles taken at random from the 360 hourly model values in the history window. Three groups of seed profiles were chosen to demonstrate the effect of data frequency in the assimilation experiment. The first group consisted of only five profiles during the 15-day period. A random number generator was used to select five integers between 1 and 360 (Appendix B). Each random integer was then identified by the corresponding Julian day and hour. Other groups of 15 and 30 seed profiles were also chosen at random from the 360 available in the window, and their respective dates and times were stored.

The model was initialized with the 1 January temperature structure at OWS PAPA for each of the 14 years used in this experiment. The predicted temperature structure was stored from the beginning of the history window (0000 GMT Day 35). In addition, the existing temperature profiles were stored every three hours in the history window, and the layer depth and temperature predictions were stored every three hours in the forecast window. These 120 values of mixed layer depth and temperature between Day 50 and Day 64 were later used as the control forecast.

B. ADDITION OF RANDOM ERRORS

Several statistics calculated from the temperatures and depths in the history window were used to estimate realistic random errors to be added to the seed profiles. The mean

and the standard deviation of the 3-hourly values of mixed layer depth and temperature in the history window were calculated. In addition, the mean and standard deviation of temperature were calculated at 2 m depth intervals from 1 to 199 m in the history window. For comparison, the mean and standard deviation of layer depth and temperature were calculated for the three-hourly forecast window values, and for the three groups of seed profiles.

Simulated temperature profiles were created using the stored seed profiles and the standard deviations of T , h , and $T(z)$ in the history window. The technique is identical to that used to create atmospheric temperature profiles for satellite data impact studies. Henry Fleming of the National Environmental Satellite Service kindly provided the code for this technique. A second call to the random number generator was used to determine random errors in mixed layer depth, and the temperature at 2 m intervals from $z = 1$ m to $z = 199$ m (Appendix C). The errors were normally distributed with a mean of zero and a standard deviation equal to the standard deviation of the appropriate history window variable. The errors were added to the seed profile as shown in Fig. 13. The new temperatures above the new layer depth were averaged to determine the simulated mixed layer temperature. Below the simulated mixed layer depth, the temperature profile was equal to the seed profile plus a temperature error at each depth. The profile was checked for stability and

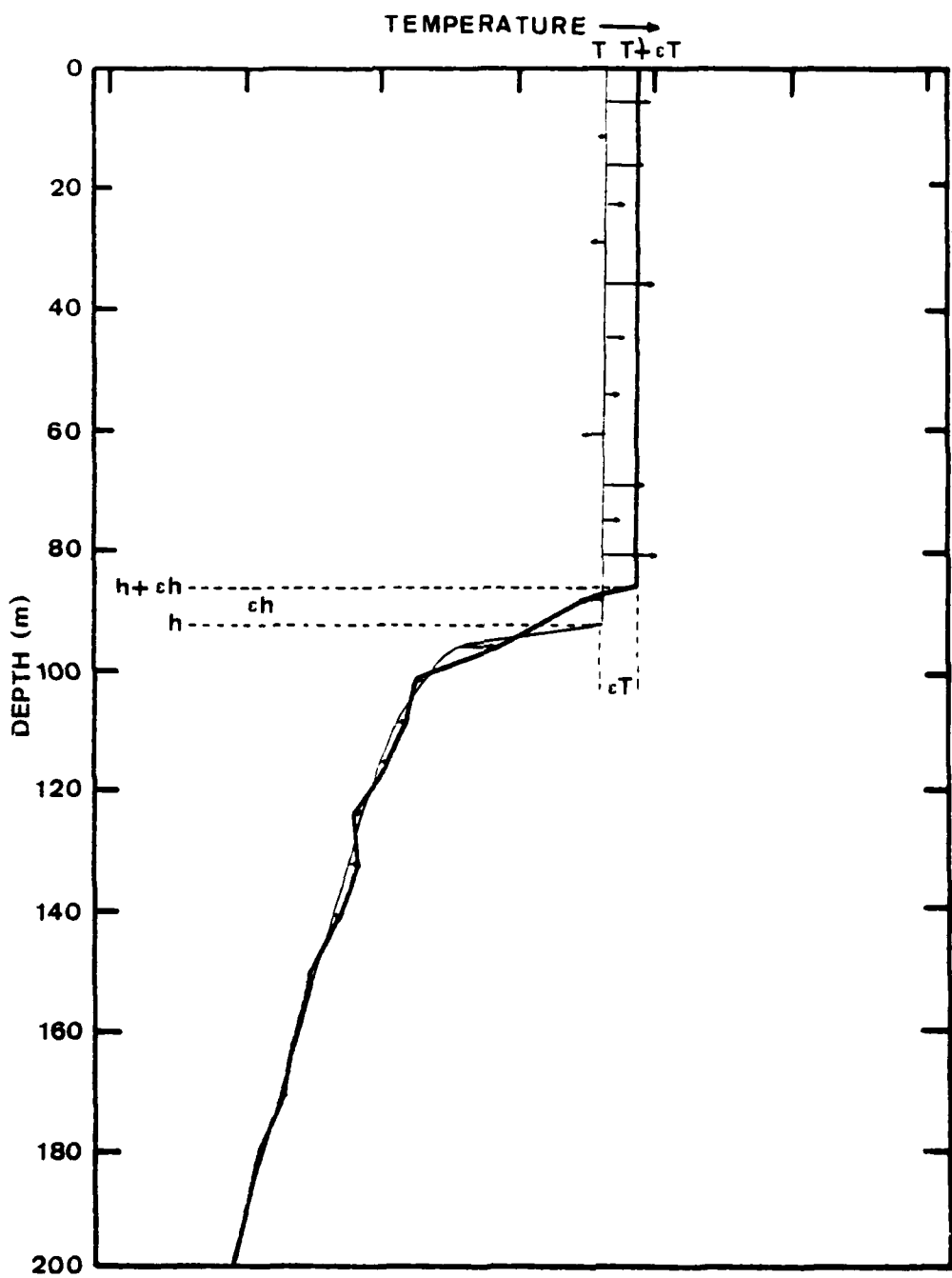


Fig. 13. Addition of random errors to seed profiles to create simulated temperature profiles. Seed profile represented by thin line, arrows represent added temperature errors, heavy line represents simulated temperature profile.

any temperature increases with depth were removed by setting the temperature at the level equal to the temperature just above it. This process was repeated for each seed profile, resulting in sets of 5, 15, and 30 simulated temperature observations in the 15-day history window.

C. ASSIMILATION OF SIMULATED TEMPERATURE OBSERVATIONS

As discussed in Chapter I, one-dimensional prediction models have the property of "perfect assimilation," that is, prior temperature structure is completely "forgotten" when a new profile is inserted. Therefore, it was not possible to directly blend the simulated profiles into the model integration as is done in atmospheric data assimilation. Rather, each profile from the history window was used to produce an estimated T profile at the beginning of the forecast window. These profiles are then combined to get a "best" estimate of initial conditions using all available observations.

The model was restarted at the beginning of the history window (0000 GMT Day 35) and run to the time of the first simulated observation. The new profile was inserted and the run continued to the beginning of the forecast window (0000 GMT Day 50). The temperature profile forecast for this time was stored and the model again reset to the beginning of the history window. This process was repeated for each of the profiles in the sets of 5, 15, and 30 simulated profiles. Thus, 50 estimates of the thermal structure at

the beginning of the forecast window were available. A schematic drawing of the forecast paths for the set of 5 profiles is shown in Fig. 14.

D. FORECASTS BASED ON AVERAGES AND SCREENED AVERAGES

The "assimilated" temperature profile to be used to initialize the model was calculated by two methods of time-weighted averaging. The weighting factor was inversely proportional to the elapsed time between the simulated observation and the beginning of the forecast window. Thus, simulated profiles near the end of the history window would be given a weighting factor of nearly 1.0, whereas a profile from early in the 15-day period would be given a weighting factor of approximately zero.

In the first case, all 5 (15, 30) of the 0000 GMT Day 50 assimilated profiles were averaged. The predicted layer depths were averaged to determine the initializing h , and the temperatures every 2 m from 1 to 199 m were averaged also. Above the new mixed layer depth, the new temperatures were vertically averaged to determine the new mixed layer temperature.

In the second case, the profiles were screened to eliminate obviously erroneous data before averaging. This procedure would be similar to a "gross-error check" in an operational analysis technique. The simulated profile layer depths and layer temperatures were compared to the mean h and layer T in the history window. If either value differed from the

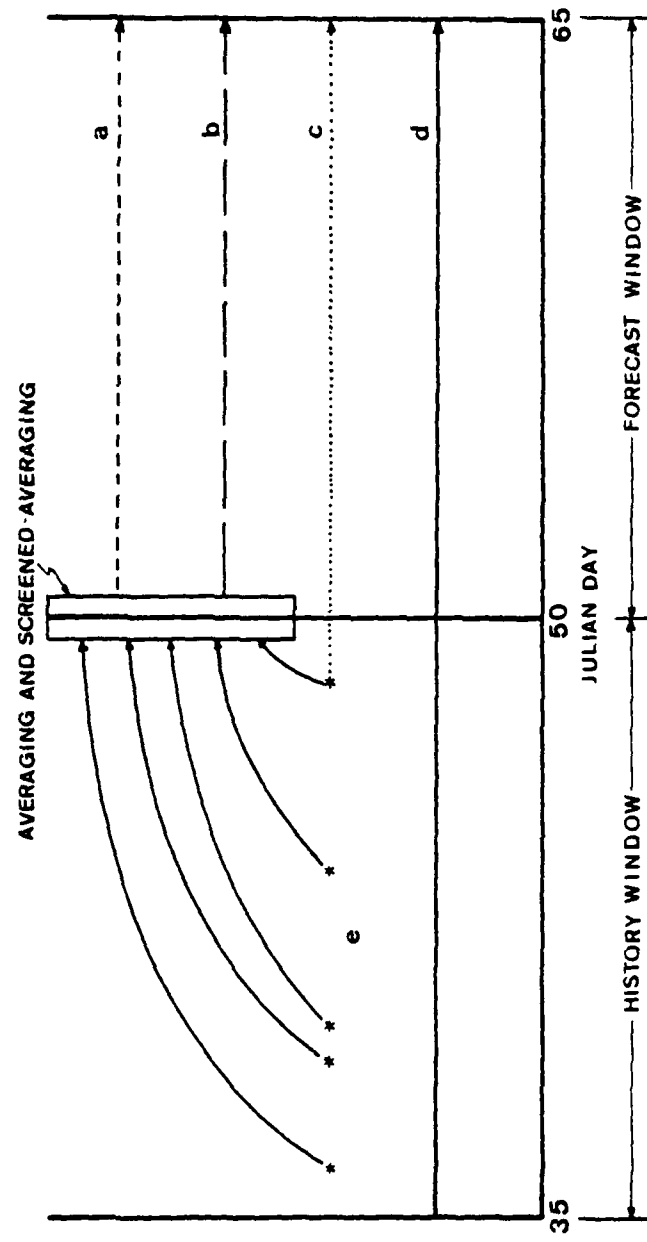


Fig. 14. Forecast paths for a winter regime study using five simulated temperature profiles. Forecasts based on the screened-average of observations (a), the average of all observations (b), and on the last available profile only (c), and the control run (d). Location of simulated temperature profiles represented by stars (e).

mean by more than two standard deviations, that simulated profile was not used in the averaging for the sets of 5, 15, and 30. The screening process removed approximately 27 percent of the profiles from the overall sample.

The model was run from Day 50 to Day 64, starting from each averaged and screened average initializing profile as illustrated in Fig. 14. Mixed layer depth and temperature forecasts were stored every 3 hours. In cases in which the assimilated profile was chronologically the last of a group (5th of 5, 15th of 15, or 30th of 30), the model run was resumed after the 0000 GMT Day 50 profile was stored. Mixed layer depth and temperature predictions based on these three simulated observations were also stored every three hours in the forecast window. Thus, there are three model predictions for each of the sets of 5, 15, and 30 original simulated profiles. Since the identical model forcing is used in each case, the differences in the predictions must be due to the number of available observations or to the use of screened versus unscreened simulated profiles.

E. ERROR CALCULATIONS

Three-hourly values for Days 50 to 64 (120 layer depths and 120 layer temperatures) were available for the ten runs: the last of the sets of 5, 15, and 30 simulated profiles; the average of the sets of 5, 15, and 30; the screened average of 5, 15, and 30 simulated profiles; and the control. Root-mean-square (RMS) and bias errors in layer temperature

and layer depth at each 3-hour time step for each of the nine forecasts were calculated. Depth and temperature errors were plotted versus forecast time for each year to compare the sets with 5, 15, and 30 simulated profiles.

A total of fourteen tests were run using OWS PAPA data from 1953-1969. Due to problems in reading the forcing files for 1954, 1959, and 1966, these years were not included in the experiment. An ensemble (14-year) average RMS error in layer depth and temperature was calculated at the 120 3-hourly time steps for each of the nine prediction methods. A 15-day average of the RMS and bias errors in h and T was also calculated for the nine methods for each year of the experiment. These ensemble average errors were used to estimate the relative effectiveness of the different forecast methods.

IV. RESULTS OF FOURTEEN PREDICTION YEARS

A. RESULTS FROM INDIVIDUAL YEARS

Examination of error plots from the fourteen years indicated three distinct categories. In eight of the years the depth and temperature errors were small in magnitude throughout most of the forecast period. In four of the years the forecast depths were consistently too large during the entire 15 days, and during the remaining two years, the predicted depths were too small.

1. Small Error Years

This category represents more than half the years in the study. The characteristic that differentiates these years from the years in the other two categories is that the errors in layer depth were small or zero for most of the period.

Layer depth errors based on the set of 15 simulated observations in 1962 are shown in Fig. 15. Plots of the forecasts based on the sets of 5 and 30 simulated profiles for 1962 were quite similar to Fig. 15. The maximum depth error of 35 m occurred in the prediction that is begun from the averaged profile at about 1200 GMT on Day 50 (0200 local time). A second maximum error of 10 m occurred a day later. From Day 52 to Day 64 the predicted depths were essentially identical to the control run with the exception of several -8 m errors in the forecast based on the last of the 15

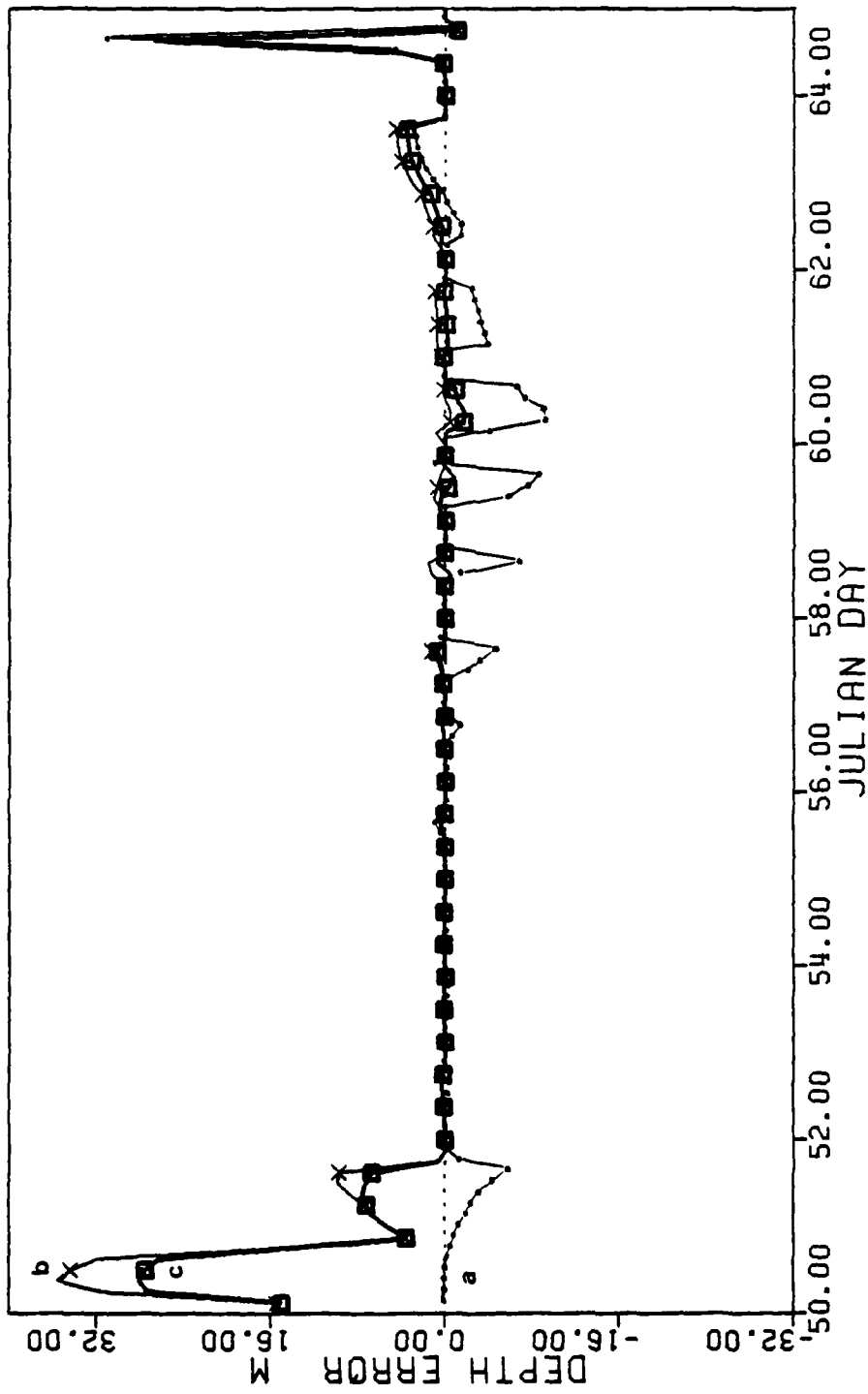


Fig. 15. Errors in forecasts of mixed layer depths for 1962 from predictions based on the last of 15 simulated profiles (a), the average of 15 simulated profiles (b), and the screened-average of 15 simulated profiles (c). Divisions on the time axis are 0000 GMT of Julian Day. Positive error represents layer depths forecast larger than control run depth.

simulated observations. A sharp peak in layer depth error was noted at 0500 local time on Day 64. Overall RMS and bias errors from the 1962 layer depth forecasts are shown in Table 5. Note that none of the forecasts in this first category were improved by averaging (screened or unscreened) the "history" profiles. It was also noted that the bias errors that were negative in the forecasts from the last of the groups were positive in forecasts made from the average and screened-average. This indicates that the averaging techniques may have caused the model to predict depths which were too large.

Layer temperature errors for the same forecasts are shown in Fig. 16. The largest (maximum of -0.06°C) errors occurred immediately after insertion of the averaged or screened-average profile. After a 30-hour period of adjustment, the temperature error became nearly constant in the averaged and screened-average runs until Day 63 when the temperature error in all three forecasts increased in magnitude. The Day 63 change, which took place over a 30-hour period, occurred during the time when the 1962 control run reached the largest depths of the forecast period.

Temperature errors in the small error cases remained nearly equal to the initial error during the parts of the forecast in which the layer depth errors were small. The part of the forecasts in this category which failed to meet the minimal-error criteria most often occurred in the first 48 hours. After adjustment to initial errors all methods

Table 5

RMS and bias errors (meters) for nine methods of forecasting mixed layer depth, based on 3-hourly predictions over a 15-day period at OWS PAPA in 1962

<u>No. of Profiles</u>	<u>Last</u>	<u>Average</u>	<u>Screened Avg</u>
RMS	5	4.8	6.3
	15	3.8	7.1
	30	3.1	5.5
BIAS	5	-0.6	1.5
	15	-0.7	2.4
	30	0.4	1.6

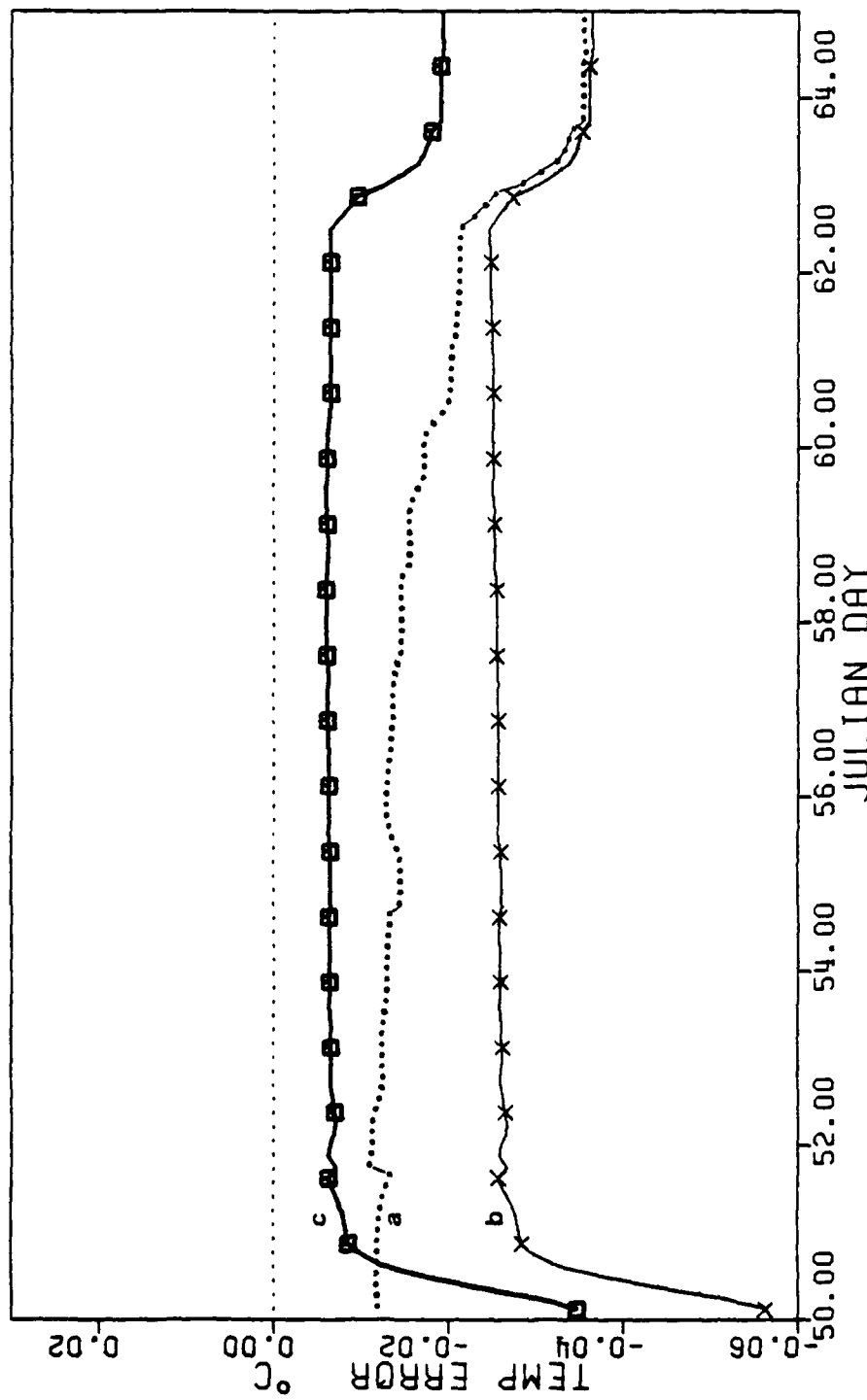


Fig. 16. Errors in forecasts of mixed layer temperatures for 1962 from predictions based on the last of 15 simulated profiles (a), the average of 15 simulated profiles (b), and the screened-average of 15 simulated profiles (c). Divisions on the time axis are 0000 GMT of Julian Day. Positive error represents layer temperatures forecast larger than control run temperature.

of forecasting resulted in excellent predictions. A second period ranging between 6 and 48 hours that had significant depth errors occurred during four of the eight years. Depth errors in this category, though small, were nearly always positive (forecast depths too large), especially in the forecasts made from averaged and screened-average simulated profiles.

2. Positive Depth Error Bias Years

Errors in predicted layer depth for the 15 simulated profile experiment in 1956 are shown in Fig. 17. The plots based on 5 and 30 simulated profiles were very similar to Fig. 17. The maximum depth error found in the entire fourteen years of the study (+79 m) occurred at 0900 GMT on Day 53 in the forecast based on the last profile of the set. This error occurred during a period with very large (greater than 130 m) layer depths which extended from Day 50 to 1800 GMT on Day 52. The 1956 control layer depth then decreased to 59 m in 3 hours, before gradually deepening to 88 m at the time of the maximum error. The layer depth predicted by the last of the set of 15 profiles increased rapidly to 167 m in the same 12 hour period. As in the tests described in Chapter II, a forecast based on an initial layer that is too deep will tend to predict depths that are too large whenever forcing causes the layer to deepen. In this case, the initial depth was greater than 160 m. When the layer retreated, the water column from 60 to 160 m was nearly isothermal. Thus, a small amount of turbulent mixing was

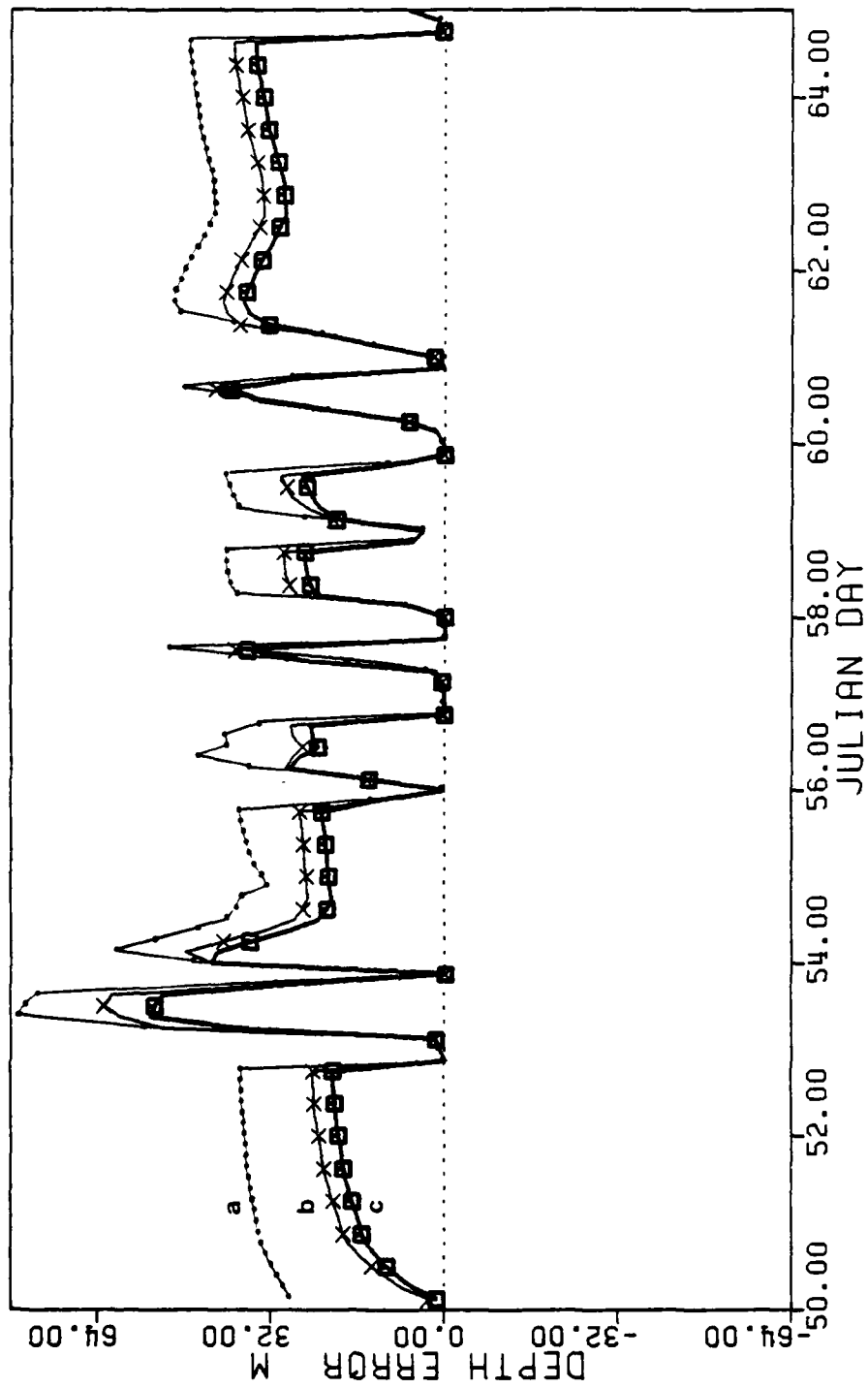


Fig. 17. Similar to Fig. 15, except for 1956.

sufficient to again cause the predicted layer depth to be excessive after the surface flux turned upward.

During the remainder of the 15-day period the errors in layer depth prediction averaged about 33 m for the last of 15 profiles, 29 m for the prediction started from the average profile, and 28 m for the prediction based on the screened-average profile. The errors near local noon were reduced to near zero for all predictions on the nine days when afternoon shallowing occurred in the control run. Similar error patterns and magnitudes were found in the 5 and 30-profile sets from 1956. Overall RMS and bias errors in the layer depth predictions are given in Table 6. In this category, inclusion of the additional information based on the "history" profiles improved the forecasts. Screening these profiles before averaging resulted in further improvement in all sets.

Temperature prediction errors for the 1956 forecasts are plotted in Fig. 18. The overall magnitude of the errors is less than 0.15°C for all forecasts. This was expected based on the results of the Chapter II experiment which showed that winter regime layer temperatures which are initially close to the control will remain close. The predictions based on the averaged and screened-average profiles started with a layer temperature that was too high, but a rapid decrease during the first 36 hours of the period reduced the screened-average forecast error to near zero and made the averaged forecast error negative. From Day 54 on,

Table 6
Similar to Table 5, except for 1956

<u>No. of Profiles</u>	<u>Last</u>	<u>Average</u>	<u>Screened Avg</u>
RMS	5	33.7	26.8
	15	36.7	28.0
	30	27.9	26.6
BIAS	5	29.8	22.9
	15	31.9	23.8
	30	24.0	22.8

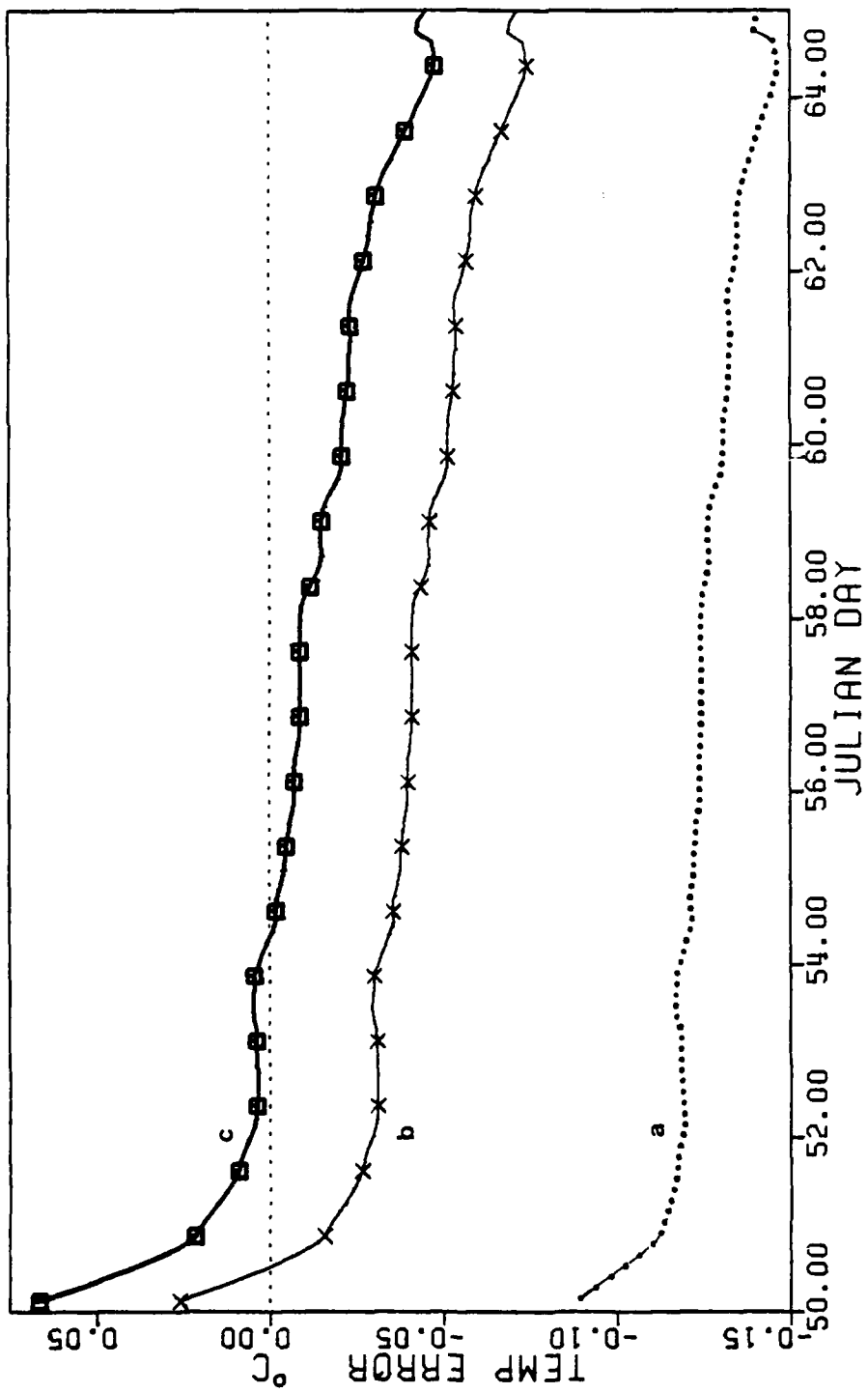


Fig. 18. Similar to Fig. 16, except for 1956.

the errors in all three temperature predictions became more negative, and reached the largest negative magnitudes several hours before the end of the period.

In the four years in which the depth errors were predominantly positive, the errors remained between zero and +80 m after Day 52. Any negative depth errors that were present at the beginning of the forecast soon became positive. Negative temperature errors (forecast temperature too low) accompanied the depth predictions that were too large. Forecasts which began with positive temperature errors changed to nearly correct predictions or negative T errors within the first 48 hours of the forecast period. This characteristic was present in every forecast made during the four years in this category.

Depth errors in this category exhibited a diurnal tendency. The errors were reduced to near zero around local noon on nine to twelve days in each year. The length of time during which the predictions were nearly correct was usually short (less than 6 hours). As described in Chapter II, the predicted layer depths during layer retreat episodes depend more on the atmospheric forcing than on the existing temperature profile in the model. For this reason, all the predictions tend to agree with the control run around local noon when layer retreat occurs.

3. Negative Depth Error Bias Years

Only two of the years (1958 and 1965) during the study had forecasts of layer depths that were too small.

Errors in predicted layer depth for the set of 15 simulated profile experiment in 1965 are shown in Fig. 19. The prediction based on the last of 15 profiles started from a layer depth 17 m too small, and the averaged profile depth was initially 10 m too large, while the screened-average profile layer depth was too small by 5 m. By the afternoon of Day 51 all depth predictions were nearly correct. From this time on, the depth errors were predominantly negative. Small positive errors (less than 10 m) occurred on Days 56-58. The daily error maxima averaged around -22 m in the forecast from the last of the 15 profiles, -16 m in the averaged forecast, and -14 m in the screened-averaged forecast. On the last three days of the forecast depth errors in the screened-average case exceeded those for the averaged profile case. Overall RMS and bias errors for the 1965 layer depth forecasts are shown in Table 7. Inclusion of the additional information available in "history" profiles reduced errors by as much as 67 percent. Screening the profiles before averaging produced further improvement, except in the 5-profile case.

Errors in layer temperature predictions in the 1965 15-profile forecasts are shown in Fig. 20. Errors in the forecasts based on averages (screened and unscreened) were small (less than 0.04 °C) and became more positive as the forecast progressed. The one exception was in the layer temperature forecast based on the last of the set of 15 simulated profiles (not shown). This temperature forecast was nearly 0.7°C too high (maximum temperature error found in

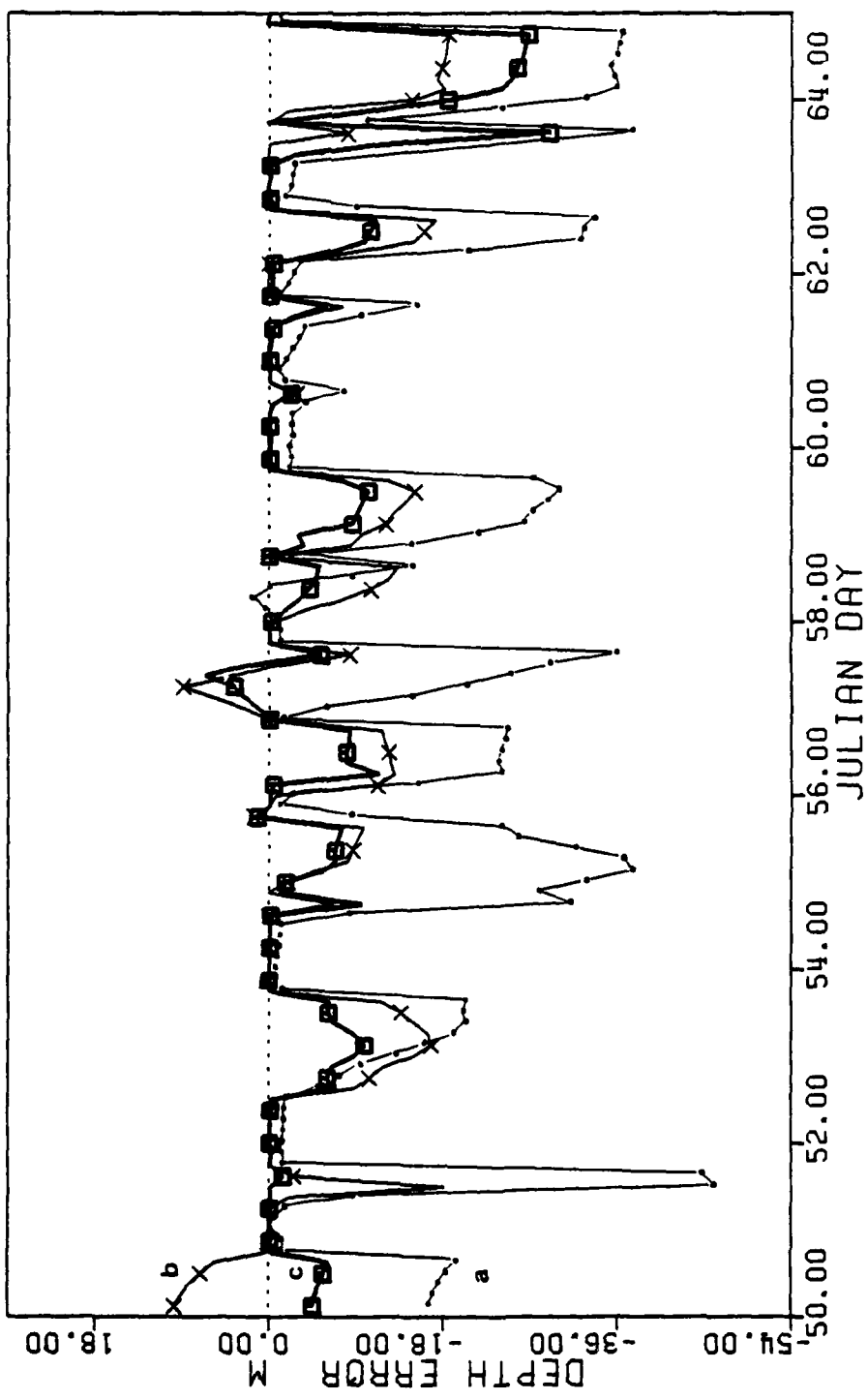


Fig. 19. Similar to Fig. 15, except for 1965.

Table 7
Similar to Table 5, except for 1965

<u>No. of Profiles</u>	<u>Last</u>	<u>Average</u>	<u>Screened Avg</u>
RMS	5	17.1	11.1
	15	19.0	8.4
	30	27.5	10.6
BIAS	5	-10.3	-6.7
	15	-13.7	-4.5
	30	-19.3	-5.7

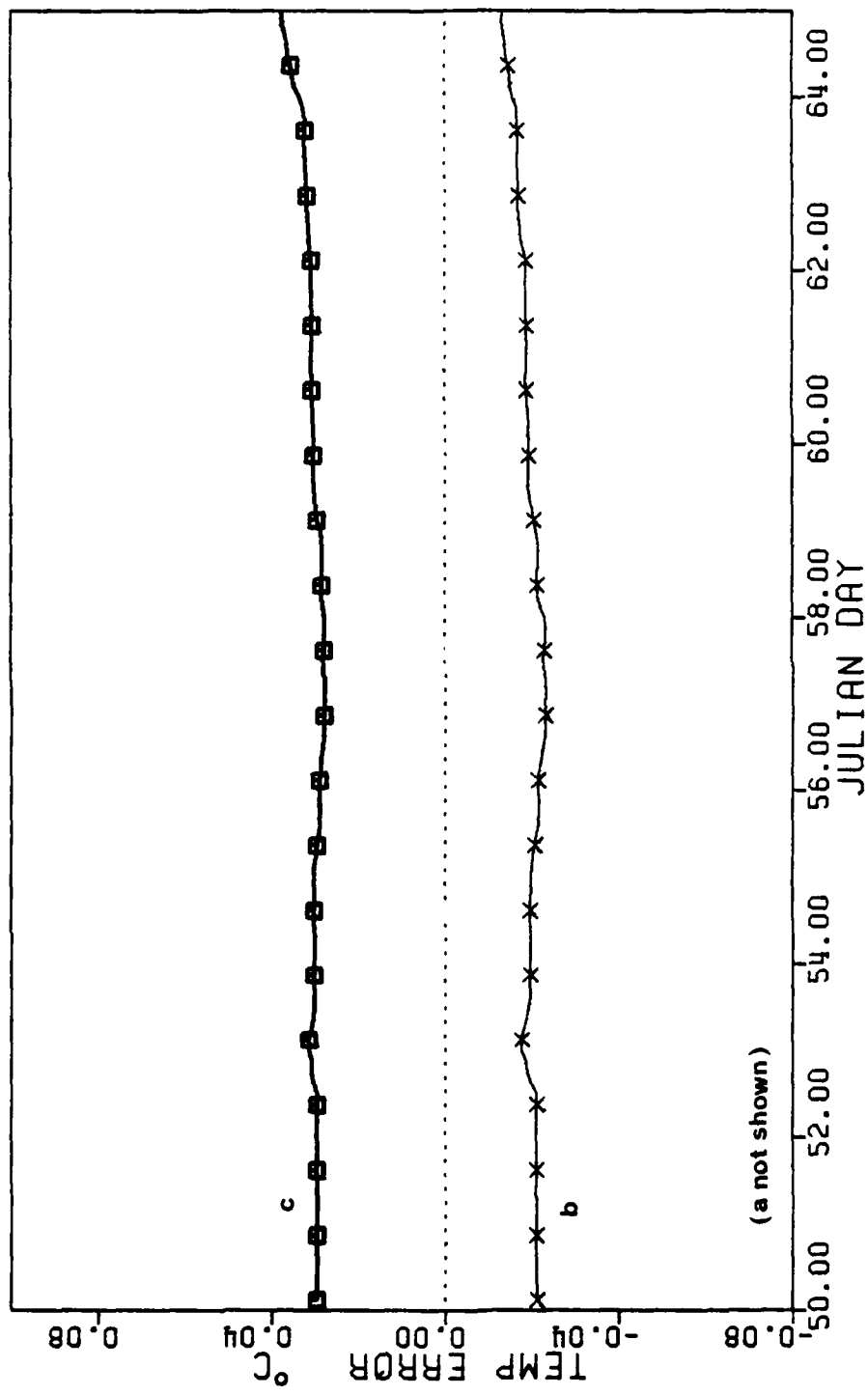


Fig. 20. Similar to Fig. 16, except for 1965.

the study). The error was caused by an artificially deep simulated profile at 2000 GMT on Day 49. Had a "gross-error check" been done on the last profiles of the group, this profile would not have been used. As the layer depth decreased, conservation of buoyancy required an increase in layer temperature, creating the warm bias.

Predictions of layer depth that were too small were unusual during this study. Even in the eight "small-error" years, the sign of the depth error was nearly always positive. However, for the two years in this category, depth forecast errors were predominantly negative after an 18 hour adjustment period. In both years, positive errors of small magnitude and short duration occurred in the middle of the forecast. As in the positive depth error category, the layer depth errors displayed a diurnal variation. Near local noon on 11 days in each year the errors were reduced to near zero.

With the exception of the forecast based on the last of the set of 15 profiles in 1965, layer temperature errors in the negative depth error category tended to be small and become more positive with time. As the forecast progressed, positive temperature errors increased in magnitude and negative errors became less negative or became positive. As in the other cases, the layer temperature forecasts in this category maintained their position relative to each other throughout the forecast.

B. RESULTS BASED ON FOURTEEN YEARS

In each of the 14 years, a similar pattern of errors existed for all nine forecasts, indicating the strong dependence of the predictions on the atmospheric forcing. Positive layer depth errors (predicted depth greater than the control) tended to be accompanied by negative (less than the control) temperature errors. This is indicated by an overall bias of +4.0 m in layer depth predictions and -0.034°C in temperature predictions. The correlation between the predicted values of h and T was $-.25$ for the 14 years. As explained by Garwood [1977], this is due to the conservation of buoyancy in the model. As the downward heat flux at the sea surface is confined to a shallower layer, the layer temperature increases proportionally. Upward heat flux at the surface, often accompanied by mechanical mixing, results in increased h and decreased layer T . When an error in depth or temperature (either too large or too small) was established in a forecast, it tended to remain for the rest of the period.

One of the primary questions raised during this study was the cause of the distinct differences between "too deep" and "too shallow" cases. It was hypothesized that the difference in the cases was caused by the character of the atmospheric forcing during the years. Examination of the layer depths in the fourteen control runs revealed that the range between depth minima and maxima tended to be larger in the runs with significant errors. This did not explain why some

of the significant errors were positive and the others were negative. A major difference in the layer depth patterns of the two groups was found in the first 84 hours of the forecast period. In each of the years in which depths were predicted to be too large, a prolonged period of strong mixing was present between 0000 GMT on Day 50 and 1200 GMT on Day 54. The atmospheric forcing caused a sustained period of layer depths of 125 m or greater (Fig. 21). The control layer depth in 1961 increased from 20 m to 100 m in the first day of the forecast. The depth remained about 125 m for 24 hours before shallowing to 50 m at 0000 GMT on Day 53. Another 30-hour period in which the layer remained deeper than 125 m occurred beginning at 0600 GMT on Day 53. In 1969, another positive error year, the layer depth was greater than 110 m from the beginning of the forecast until Day 54.

In the negative depth error cases, large layer depths (greater than 110 m) around 0500 local time alternated with smaller depths (30 m or less) near local noon during the first four days of the forecast. This condition is indicative of a nearly isothermal upper 100 m. Downward surface buoyancy flux during the afternoon results in a shallow layer with increasing temperature. This transient feature disappears when the flux is upward at night. The 1958 and 1965 control depths displayed this deep-shallow alternation for the first 84 hours of the period (Fig. 21). In years in which the atmospheric forcing did not cause either the

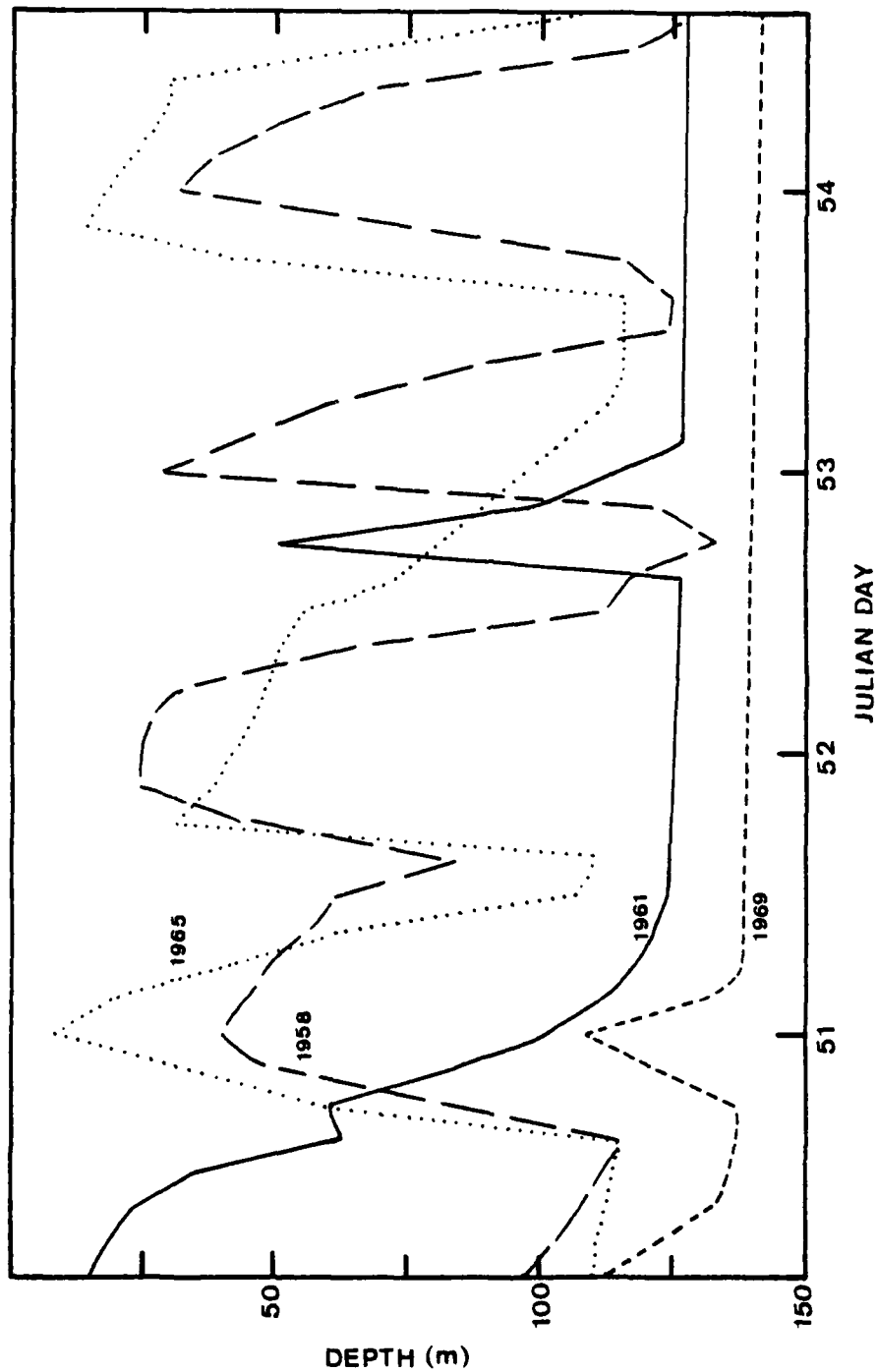


Fig. 21. Model-predicted mixed layer depths for Julian Days 50-54 for control runs in 1958, 1961, 1965, and 1969. Divisions on the time axis represent 0000 GMT of Julian Day.

deep-shallow alternation or an extended period of large layer depths near the beginning of the forecast, large errors did not occur.

As described in Section IV.A, decreases in layer depth error around local noon were found about 70 percent of the time in all forecasts. This diurnal tendency was evident in the plot of ensemble RMS depth error for the fourteen years (Fig. 22). Minima in RMS error occurred around local noon on all 15 days, whereas the maxima occurred around 0200 local time. Average depth error maxima were 20 m for the forecasts based on the last of the set of 30 simulated profiles, 18.5 m for the predictions from the average of the 30 profiles, and 17.5 m for the screened-average of 30 profiles forecast. Average depth error minima were 9 m, 8 m, and 7.5 m, respectively.

No diurnal variation was evident in the ensemble mean temperature errors (Fig. 23). The errors in prediction of layer T tended to increase as the forecast progressed, but remained small throughout the period. The temperature forecasts from the averaged and screened-average profiles showed improvement during the initial 18 hours of the forecasts.

On the first day of the forecast period, the layer depth forecast based on the last simulated profile was better than the two averaging techniques. However, the averaging procedures generally improved the forecast after a 15-hour adjustment period. Ensemble RMS and bias errors in layer depth predictions for the study are given in Table 8. Overall

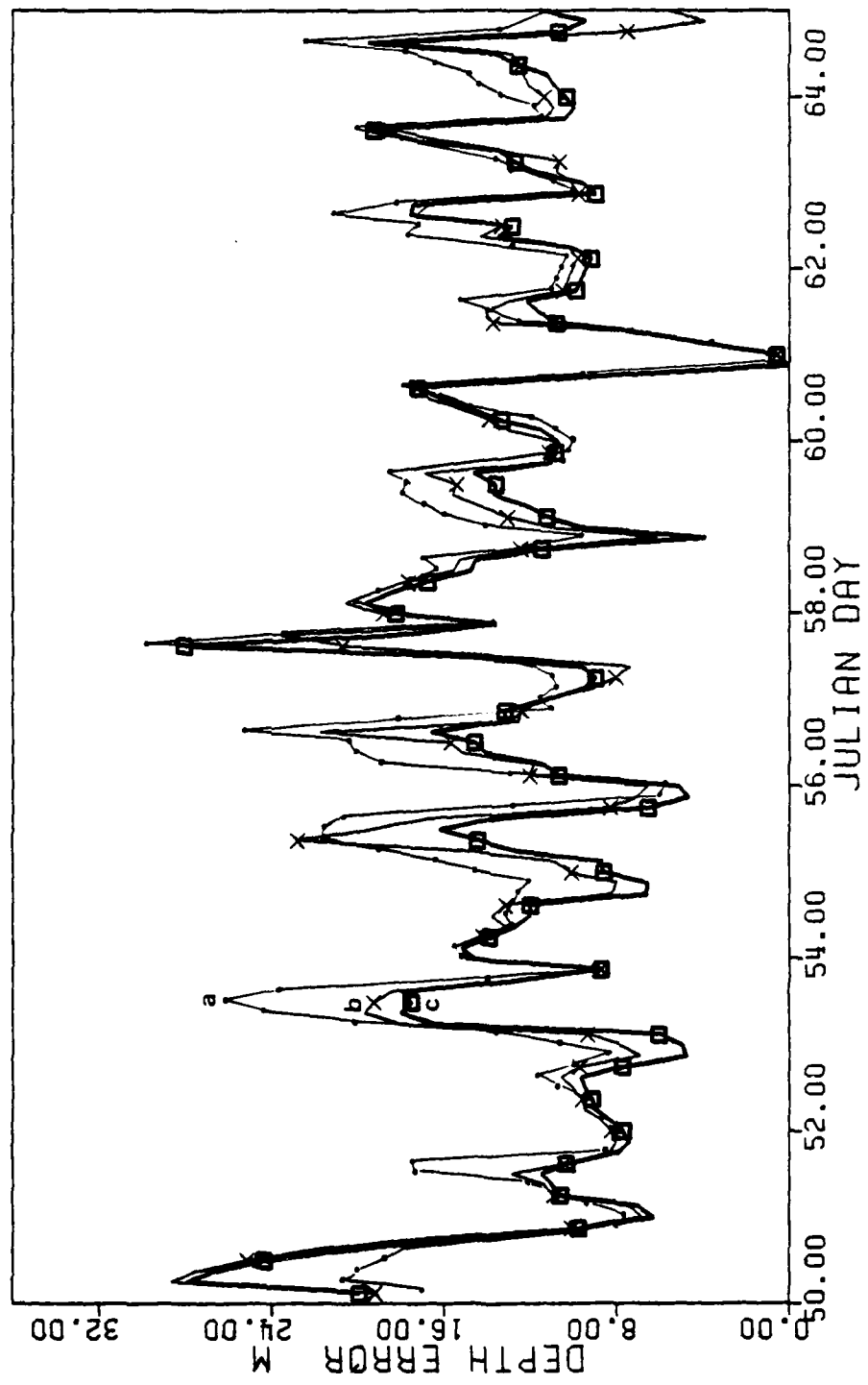


Fig. 22. Root-mean-square errors in predicted layer depths for ensemble of 14 years based on the last of 30 simulated profiles (a), the average of 30 simulated profiles (b), and the screened average of 30 simulated profiles (c). Time-axis divisions represent 0000 GMT on Julian Day.

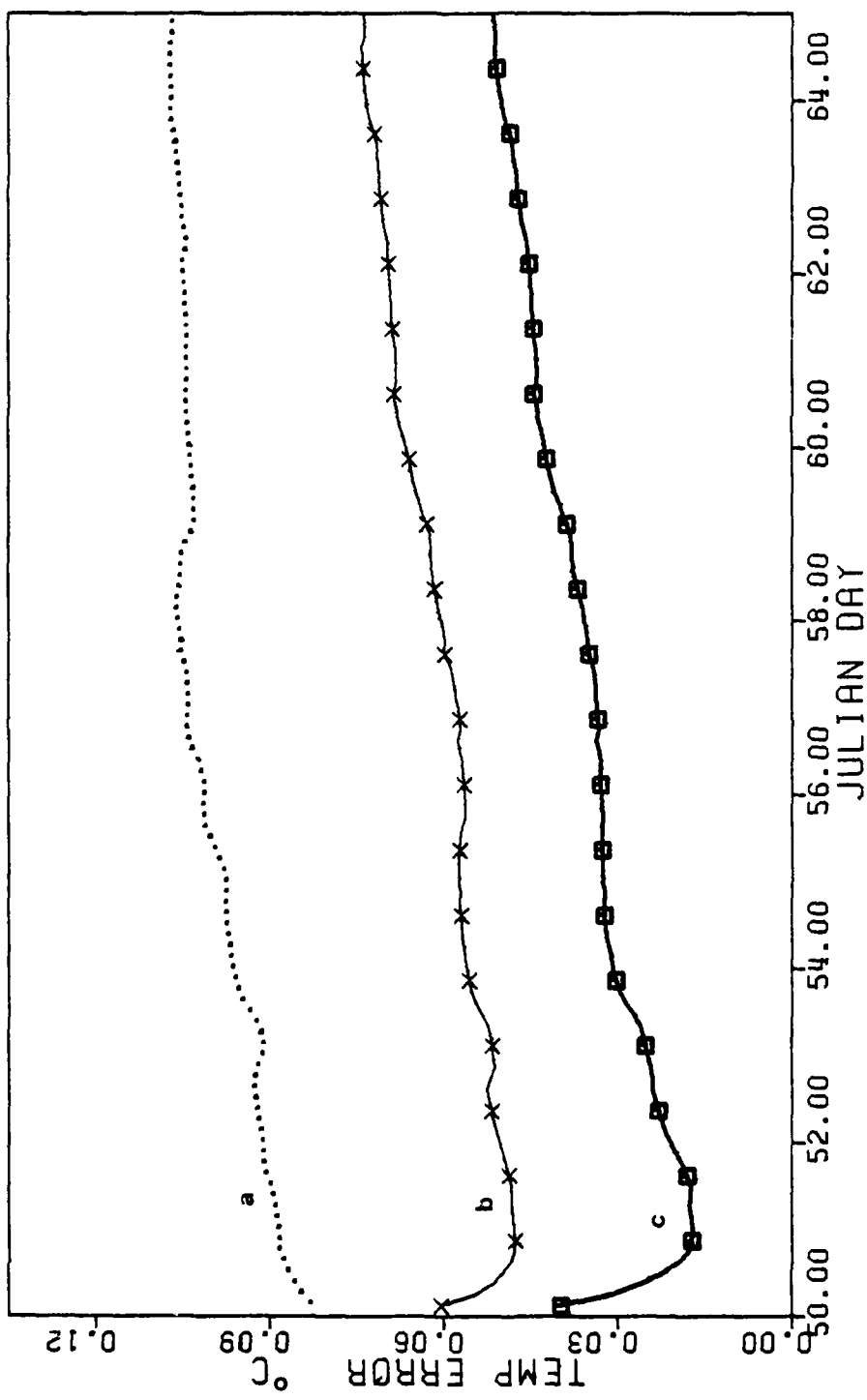


Fig. 23. Similar to Fig. 22, except for mixed layer temperature errors.

Table 8

Fourteen year ensemble of RMS and bias errors (meters) for nine methods of forecasting mixed layer depth, based on 3-hourly predictions over a 15-day period at OWS PAPA

<u>No. of Profiles</u>	<u>Last</u>	<u>Average</u>	<u>Screened Avg</u>
RMS	5	14.1	14.7
	15	15.8	14.6
	30	15.1	13.8
BIAS	5	4.1	4.2
	15	2.8	4.7
	30	2.4	5.0

reduction in RMS error was achieved through the insertion of averaged "history" profiles. Further improvement was accomplished by screening the profiles before averaging.

The bias errors in layer depth prediction presented in Table 8 show that the average and screened-average predictions resulted in an increase in the positive bias. This was due to the method used to average the profiles. While h and T were handled correctly, the averaging process tended to reduce ΔT and the gradient immediately below the layer. The weaker gradient reduced the potential energy of the water column and resulted in excessive deepening relative to the control. This implies that proper initialization of a one-dimensional ocean model requires that the below-layer T gradient be handled carefully.

Increases in the amount of temperature structure history included in the averaging techniques improved the results somewhat, but the lowest RMS error achieved by any prediction method was 12.9 m, a result of screened-averaging 15 simulated profiles. Increasing the number of history profiles from 5 to 15 improved the forecasts, but further increases in the amount of "history" did not result in significant further improvement.

V. SUMMARY

A. CONCLUSIONS

Knowledge of upper ocean conditions is important to several defense and economic interests. A prediction capability for the OPBL would be advantageous to U.S. Navy, Coast Guard, and fisheries management personnel, and may also aid in climate prediction. The Garwood OPBL model is one available tool for prediction of mixed layer depths and temperatures. A one-dimensional form of the model using data from OWS PAPA has been tested for a variety of oceanic and atmospheric forcing regimes.

The goal of this study was to improve the oceanic mixed layer forecasts by assimilating recent temperature profiles as a part of the model initialization. The first step was to test the reaction of the model to insertions of erroneous temperature profiles. Tests of model sensitivity were made for winter and summer conditions, and during the spring transition period. Layer depth predictions were not greatly affected by erroneous initial data when the layer was re-treating. When the layer was deepening, changes in the initial h , T , or ΔT (temperature jump at the base of the layer) had significant effects on the predicted layer depths. Increasing the initial T , decreasing h , or increasing ΔT caused increased stability at the base of the layer, and resulted in impeded deepening and smaller layer depths. Conversely,

decreasing T or ΔT , or increasing h caused decreased stability and facilitated deepening. Initial biases in layer temperature tended to persist throughout the 15-day forecasts. Errors in initial h can affect layer temperature forecasts. A shallow layer will result in T predictions that are too low as layer depth is corrected, while an initial h which is too large results in predictions of layer T which are too large.

Fourteen years of data were used to test the effectiveness of initializing the ocean model with profiles (simulated) from the previous 15-day period (history). Simulated temperature profiles were created by adding random errors to profiles taken from the model in the history window. The errors were normally distributed with a mean of zero and the standard deviation of the appropriate history window variable. In the first initialization technique, all available profiles were averaged with a weighting proportional to the elapsed time. In the second technique profiles were screened to eliminate gross errors before averaging. The effect of having 5, 15, or 30 profiles during the prior 15-day period was also tested.

Based on these 14 years of forecasts during a late winter period, the following conclusions were drawn:

Atmospheric forcing in the first few days of the forecast determined the character of errors in layer depth predictions. If a prolonged strong wind period during these days caused deep layers which persisted for 24 hours or more, predictions of h tended to be too large. If large layer

depths on the first four nights alternated with relatively shallow depths in the afternoons, predictions of layer depth tended to be too small throughout the forecast period. The largest errors in the mixed layer depth predictions occurred between 0000 and 0500 local time, when the layer was generally deepest.

After a one-day period of adjustment, forecasts of layer depth and temperature from averaged profiles were an improvement over forecasts based on the most recently available profile. This was especially true for years in which errors were large. Further improvement was achieved by screening available history profiles before including them in the averaging process.

Increasing the number of available profiles from 5 to 30 for use in the model initialization resulted in small improvements in the forecasts. The slight decrease in depth prediction errors by increasing the number of history profiles from 15 to 30 may not be worth the increased computer time required to prepare the larger initialization. This lack of improvement may be partly due to the inverse time-weighting process.

B. RECOMMENDATIONS

Before data assimilation in the Garwood model can be expanded to three dimensions, further testing should be done. It should be determined if the conclusions drawn in the winter case also hold true at other times of the year. It

is recommended that the averaging and initialization processes be tested at times other than 0000 GMT. The diurnal variation of the mixed layer depth has been shown. It is possible that initialization in a different part of the cycle could affect the above results. It is also recommended that the time-weighting of the profiles be tested. It was shown that forecast accuracy is less dependent on length of forecast than on the character of atmospheric forcing. Equal weighting of simulated profiles would not enhance the effect of inaccurate forecasts made from profiles near the end of the history window.

A final suggestion would be to change the average and screened-average techniques for computing the initial profile. In addition to layer depth, the temperature jump at the base of the layer, and/or the potential energy in the layer should be averaged. This would maintain the gradient of temperature below the layer and would reduce the excessive deepening in the average and screened-average predictions.

APPENDIX A

SENSITIVITY OF THE GARWOOD OPBL MODEL TO VARIATIONS IN VERTICAL RESOLUTION

A. REASON FOR STUDY

The Garwood oceanic mixed layer model has been used in several experiments with a depth interval of 1 meter [Elseberry and Garwood, 1978 and Elseberry, Gallacher, and Garwood, 1979]. However, bathythermograph profile temperatures are often stored at 5 m depth intervals. Although increasing the vertical interval would reduce computer requirements, it was important to determine to what extent model accuracy would be degraded by using a larger vertical interval (dz). If model accuracy decreased to unacceptable levels when dz was set at 5 m, observed profiles must be interpolated to allow better vertical resolution.

The effect of decreased vertical resolution was tested using the ocean station PAPA 1964 data. As in Chapter II, results were analyzed during the winter (Days 30-45) and summer (Days 200-215) regimes, as well as the spring transition (133-148). Variations in model resolution were made with the 1964 control data and with the DEEP profile simulations similar to Chapter II.

B. EFFECT ON RUNS WITHOUT INSERTION

Starting from the 1 January 1964 profile, the model was run through Julian Day 215 using the 1964 forcing. Runs were

made with vertical intervals of 1, 2.5, and 5 m. Model-predicted mixed layer depths are shown in Figs. 24, 25, and 26 for the winter, spring, and summer periods, respectively. The simulation with $dz = 1$ m was considered most accurate, and was used as the control. Deviations from layer depths predicted by this run were used to estimate the degradation of accuracy caused by using larger vertical spacings.

During the winter period, the simulations with 2.5 and 5 m resolution generally resulted in layer depths that were too shallow, especially during entrainment phases. Exceptions to this trend occurred on Days 32 and 41, when the depths with 2.5 m resolution were slightly deeper than the control, and on Day 34, when both the 2.5 m and 5 m resolution runs deepened more quickly than the control (Fig. 24). Throughout the 15-day period, the maximum depths in each deepening phase were reached in the control run.

During the layer retreats which occurred near local noon on 12 of the 15 days, the depths predicted by all runs were within 1 m of each other. On Days 32, 40, and 42 the minimum layer depth in the 5 m resolution run was smaller by 6-15 m than in the other two simulations. A tendency for slower deepening and smaller maximum depths is also shown in the run with 5 m resolution. The layer depths predicted in the 2.5 m resolution run were within 5 m of the control depth except on the evening of Day 42, when the predicted depth was 10 m too small.

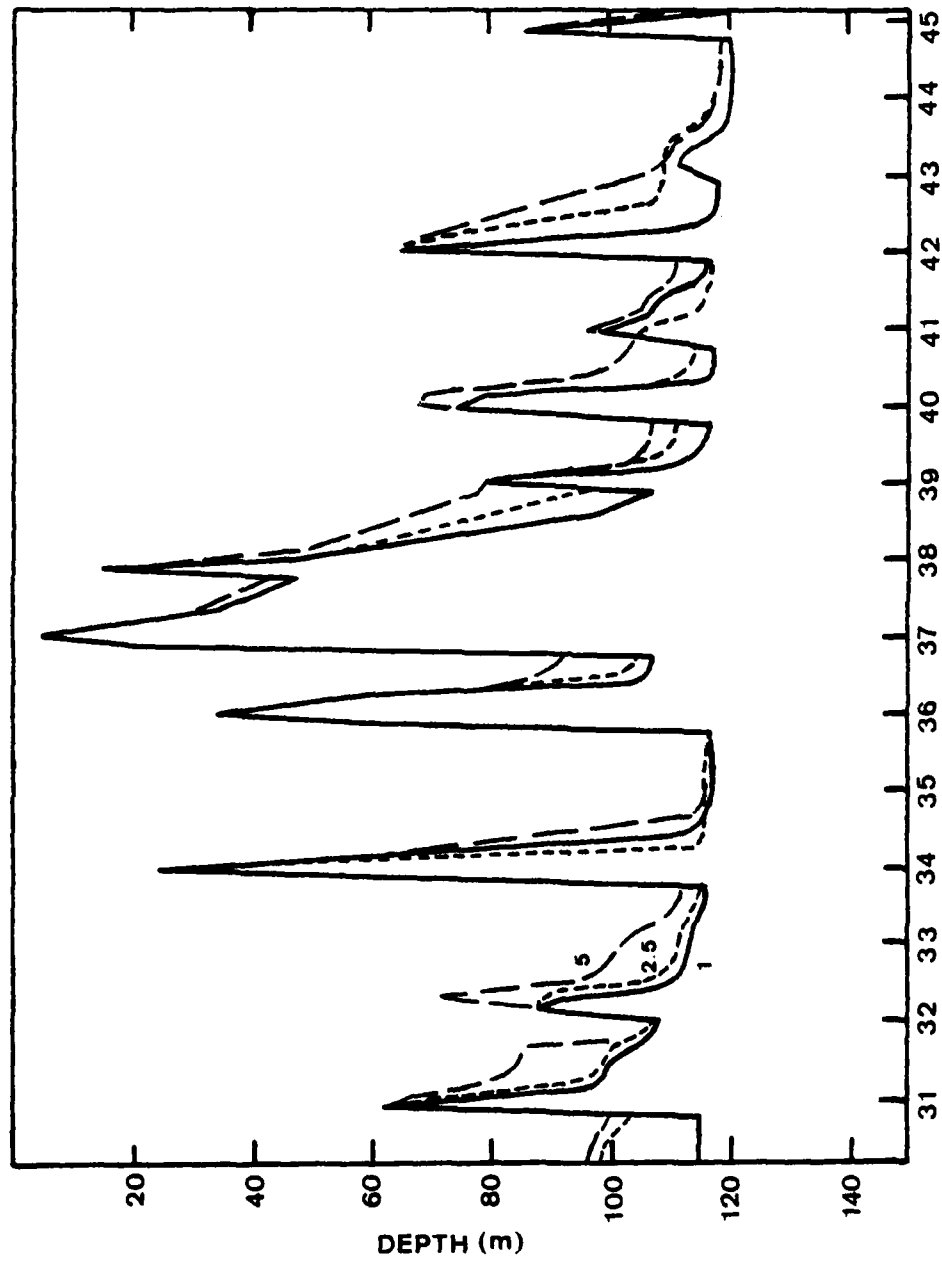


Fig. 24. Model-predicted mixed layer depths for Julian Days 31-45, 1964 at OWS PAPA. Model runs are represented with vertical resolutions of 1, 2.5, and 5 m. Time-axis divisions represent local noon at OWS PAPA.

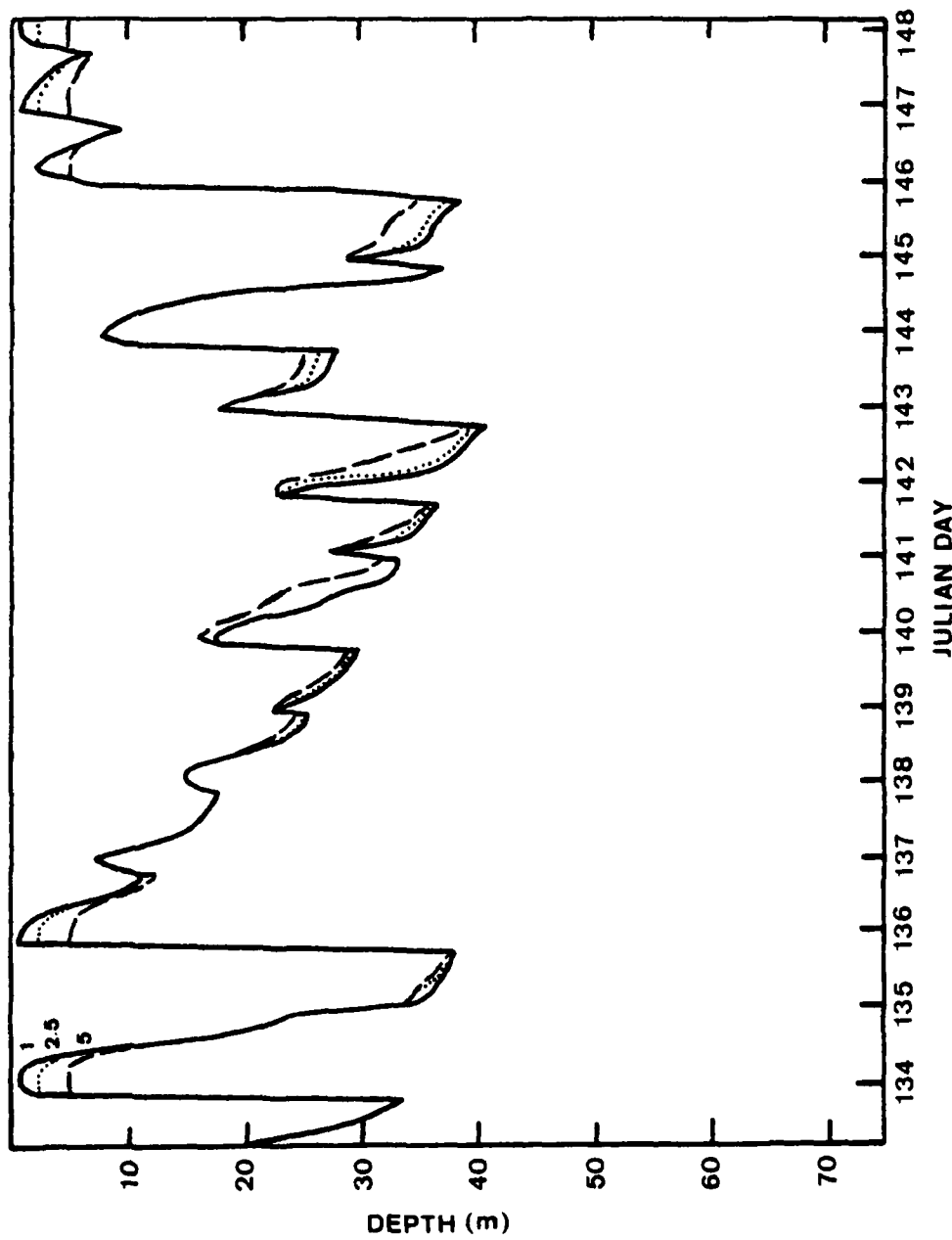


Fig. 25. Similar to Fig. 24, except for Julian Days 134-148.

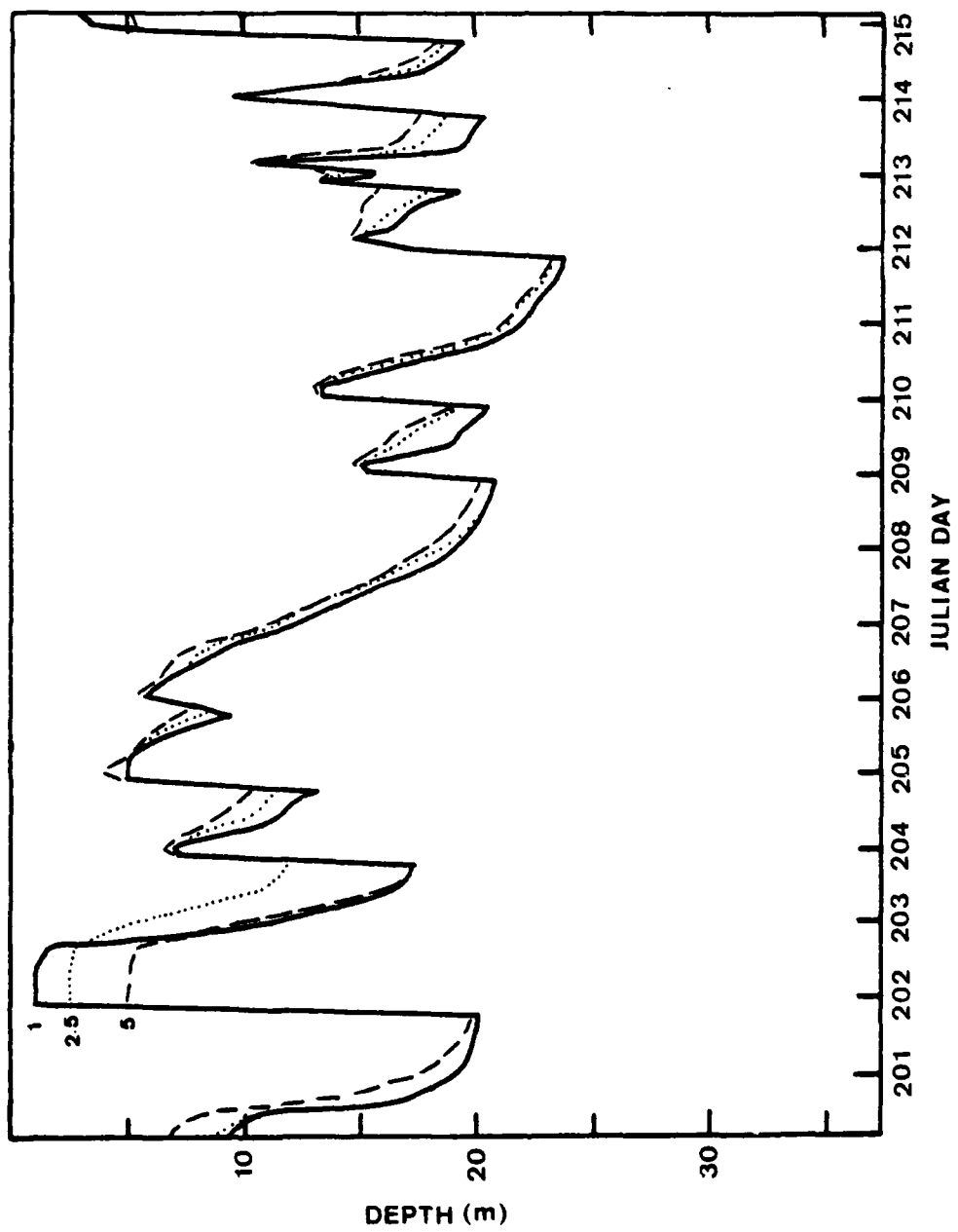


Fig. 26. Similar to Fig. 24, except for Julian Days 201-215.

During the winter regime, the predicted layer temperatures were unaffected by the change in vertical resolution. The temperatures were within 0.01°C of the control value throughout the 15-day period.

During the spring transition period, the errors in predicted layer depths were small for both 2.5 m and 5 m resolution simulations (Fig. 25). The largest errors occurred on Days 134, 136, 147 and 148, when the layer retreated to 1 m in the control run. These differences are caused by the model constraint that makes the minimum layer depth equal to one vertical interval. Thus the run in which $\text{dz} = 5 \text{ m}$ cannot predict an h less than 5 m. During the remainder of the 15-day period, the predicted layer depths with 2.5 m vertical resolution were within 1 m of the control. During deepening phases from Days 140 to 146 the layer depths with 5 m resolution were smaller than the control values, but the maximum error was only 4 m.

Mixed layer temperatures predicted for the spring period were within 0.01°C except when the layer retreated to the model minimum depth. Days 134, 136, 147 and 148 were marked by afternoon increases in layer temperature ranging from 1.0 to 1.7°C in the run with 1 m vertical resolution. Heat added to the layer from the atmosphere was distributed over a deeper layer in the other runs, and consequently, the layer temperature did not increase as rapidly. The simulated temperatures with the 2.5 m and 5 m resolutions were 0.3 to 0.6°C lower

and 0.5 to 0.8°C lower, respectively, than the maximum temperature in the control run.

The errors caused by increasing the vertical interval during the summer were also small. On Days 202, 205, and 215 the layer retreated to a depth less than 5 m. On these afternoons the model restrictions introduced a too-deep error in the 5 m simulations and on Day 202, when the control depth reached 1 m, a 1.5 m error in the $dz = 2.5$ m depths. During the remainder of the period the relationship between the simulations with different resolutions was inconsistent. The errors in the 5 m resolution case tended to be larger, but in a few cases, notably on Days 203-204, the 2.5 m resolution errors were larger, while the 5 m resolution values were close to the control (Fig. 26). As in the winter and spring periods, the errors in summer were small during the retreat phases (0.5 m) and a bit larger during deepening phases (0.75 to 4 m).

The degradation in mixed layer temperature accuracy during the summer was less than 0.2°C, except when the layer retreated to the minimum model depth. As in the spring case, this shallowing was accompanied by a rapid warming of the layer. In a case in which the control run temperature increased 1.4°C in 9 hours, the 2.5 m resolution run had a 0.6°C error, while the 5 m resolution temperature was 0.85°C too low. When the layer again deepened beyond 5 m, these large differences in layer temperature disappeared.

AD-A100 153

NAVAL POSTGRADUATE SCHOOL MONTEREY CA
DATA ASSIMILATION IN A ONE-DIMENSIONAL OCEANIC MIXED LAYER MODEL—ETC(U)
DEC 80 L L WARRENFELTZ

F/6 8/10

NL

UNCLASSIFIED

2 of 2
AD-A100 153
10-316.3

END
DATE
FILED
7-81
DTIC

C. EFFECT ON INSERTION RUNS

To further test the effect of increasing the vertical interval, runs were made in which the DEEP profile insertions from Chapter II were repeated with decreased vertical resolution. Insertions were again made on Julian Days 30, 133, and 200, but with vertical intervals of 2.5 and 5 m. The results of these runs were then compared to the DEEP insertion runs with a 1 m interval.

As in the runs without insertion, the largest layer depth error magnitudes occurred in the winter regime. Layer depths for Days 30 to 45 are shown in Fig. 27. As in the other cases, errors during shallowing phases were small, whereas errors in deepening phases and in maximum depths were larger. In nearly every instance, the layer depths with 2.5 and 5 m resolution were too small. Error magnitudes in the simulations with the insertion of DEEP profiles were larger than in the runs without insertion. The depths predicted in the 2.5 m resolution run averaged about 10 m too small in the deepest parts of the cycle. The maximum error was 30 m on the afternoon of Day 41. The errors were generally larger with the 5 m resolution, with the maximum of 34 m being observed on Day 42.

As in the runs without insertion, the winter regime mixed layer temperatures were not significantly affected by the increase in vertical interval. The errors introduced were less than 0.03°C throughout the run.

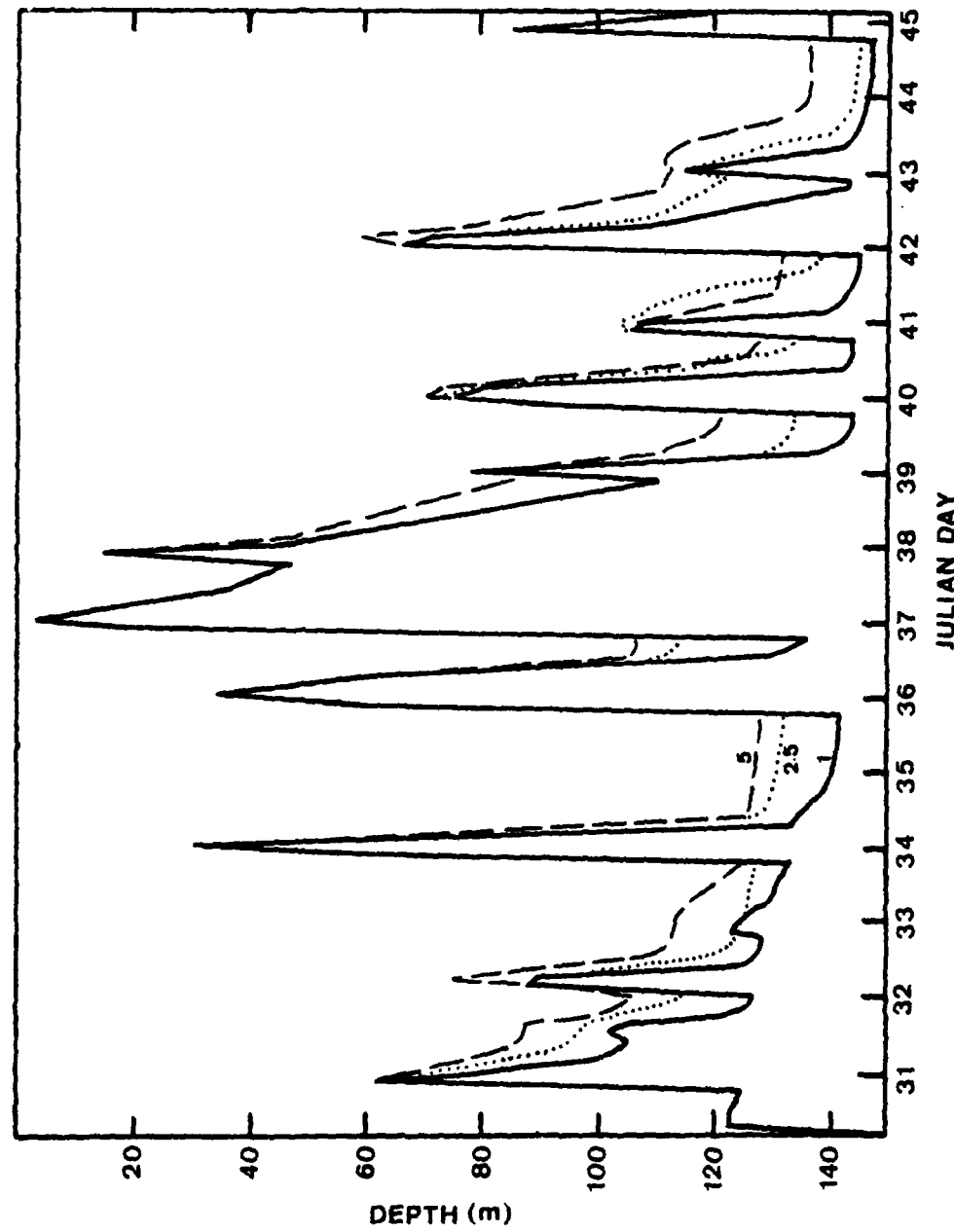


Fig. 27. Model-predicted mixed layer depths for DEEP profile insertions on Julian Days 31-45, 1964 at OWS PAPA. Model runs are represented with vertical resolutions of 1, 2.5, and 5 m. Time-axis divisions represent local noon at OWS PAPA.

The DEEP profile which was inserted on Day 133 was a good approximation of the profile it replaced (Fig. 7). The difference between them was a small increase in buoyancy between 20 and 75 m in the replacement profile, which effectively increased the layer depth to 75 m. When this DEEP profile was inserted with varying vertical intervals, the results were nearly identical to the Day 133-148 period without insertion (Fig. 25). The simulations with the DEEP layer depth retreated to 24 m during the first 3 hours, and the values with the 1, 2.5, and 5 m vertical resolutions were within 2 m of their respective non-insertion depths through the remainder of the 15-day period. The DEEP insertion mixed layer temperatures in the spring were also nearly identical to the runs without insertion.

The mixed layer depth errors in the summer for DEEP profile insertions follow a pattern similar to the runs without insertion and to DEEP profile insertions for other times of the year. The 2.5 m and 5 m resolution runs predict layer depths which are nearly identical to those with 1 m resolution during shallowing phases, and too small in deepening phases (Fig. 28). The errors are 10 and 14 m for the 2.5 and 5 m resolution simulations during the first deepening phase, but after Day 202 the maximum errors are 5 m with the 5 m resolution and 3 m with the 2.5 m resolution.

Unlike the non-insertion runs and the DEEP insertions at other times of the year, the summer DEEP profile insertions

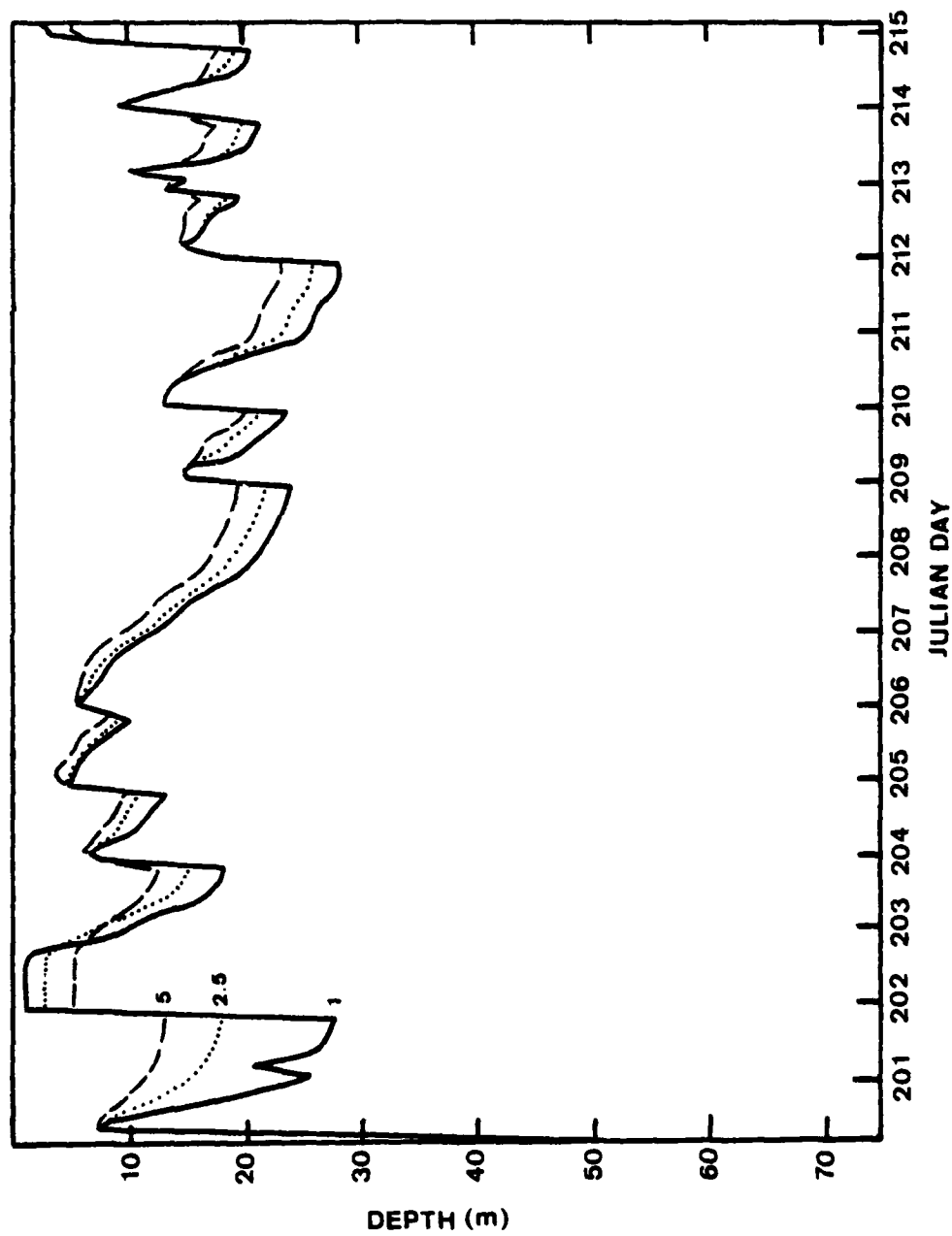


Fig. 28. Similar to Fig. 27, except for Julian Days 201-215.

result in significant layer temperature errors when the vertical interval is increased (Fig. 29). The DEEP profile that was inserted on Day 200 had a layer depth of 50 m. This depth was much too large to be maintained by the available atmospheric forcing. In the first three hour time step the layer retreated to 7.5 m. As this large retreat occurred, conservation of buoyancy and potential energy required a higher mixed layer temperature. The control run temperature increased 0.3°C to 11.9°C . In the 2.5 m resolution case, the layer temperature increased to 12.35°C , and with the 5 m resolution the temperature increased to 13.1°C . These temperature differences are due to the procedure for distributing the excess buoyancy contained in the partial vertical interval at the base of the mixed layer. Since these partial intervals may be larger when $dz = 2.5$ or 5 m, the amount of heat redistributed into the mixed layer may be larger. As was noted in Chapter II, a warm bias in layer temperature tends to be maintained for the remainder of the period. Insertions of an excessively deep profile under summer conditions results in a layer temperature which is too high (Fig. 12). If the insertion experiment is done with a model that has vertical intervals greater than 1 m, this difference is magnified.

It is concluded that larger vertical intervals can be successfully used in the Garwood OPBL model, provided the user recognizes several limitations. As shown in Table 5,

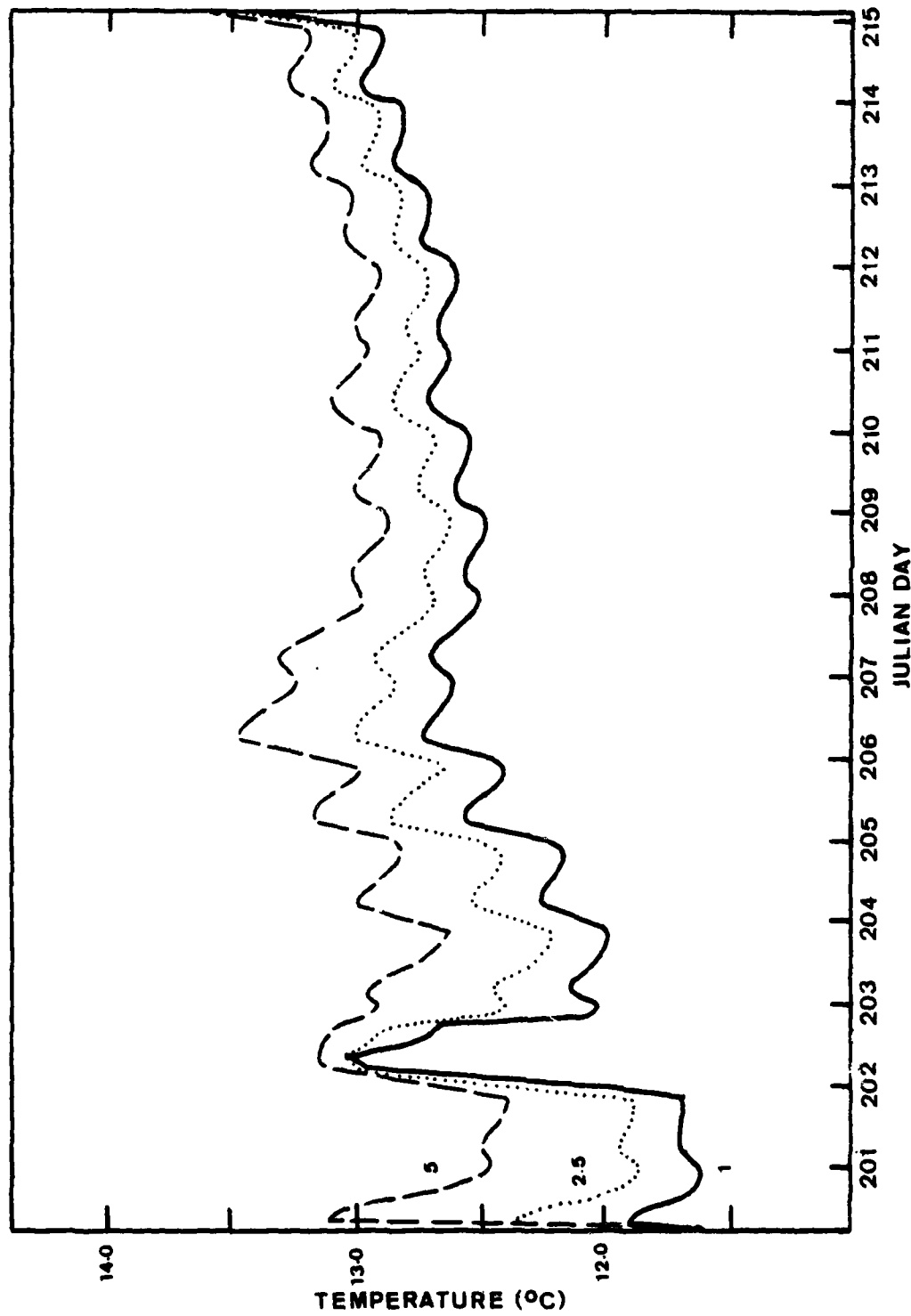


Fig. 29. Model-predicted mixed layer temperatures for DEEP profile insertions on Julian Days 201-215, 1964 at OWS PAPA. Model runs are represented with vertical resolutions of 1, 2.5, and 5 m. Time-axis divisions represent local noon at OWS PAPA.

a negative bias in layer depth is present during deepening phases and in maximum depth. This is due to the representation of the temperature jump at the base of the layer, ΔT , when the vertical resolution is decreased. For model purposes, ΔT is increased, which impedes deepening. Additionally, the minimum layer depth of the model is one vertical interval. If the simulated layer depth shallows to a value less than 5 m in a run with vertical interval equal to 5 m, the depth cannot be accurately represented. The depth in the model will be artificially large and the layer temperature will be too small.

Table 9

Summary of the sensitivity of the Garwood OPBL
model to variations in vertical resolution

Effect of increasing dz

Layer depth in the shallowing phase	Little degradation in accuracy.
Minimum layer depth	Occasionally too small, especially when dz is increased to 5 m. If layer depth is decreased to less than one dz, cannot reflect the accurate depth (minimum is too large).
Layer depth in the deepening phase	Deepens too slowly. The more dz is increased, the more slowly deepening occurs.
Maximum layer depth	Nearly always too small. Errors are larger as dz is increased.
Layer temperature	Little degradation in accuracy, except when combined with a summer profile having a layer which is too deep. In this case, resulting temperatures are too warm.

APPENDIX B

RANDOM SELECTION OF SEED PROFILES

To choose a set of times in the history window at which to simulate temperature profiles, a random number generator was called which made it possible to randomly choose any number of the 360 available profiles. When the program was started, an initial seed number (an odd integer from 1 to 999,999,999) was input. This seed number was multiplied by a random number between 0.0 and 1.0 which was obtained by calling subroutine RANDU. The resulting random number was used as the calling argument seed number in a call to IMSL subroutine GGUBS. GGUBS created a vector of 360 random numbers between 0 and 1. A second vector of 360 integers arranged in ascending order was created. Using these two vectors as calling arguments, a call was made to IMSL subroutine VSRTP, which sorted the random vector into ascending order while rearranging the integer vector. Thus, the integer vector is now a random arrangement of the integers between 1 and 360, and any number of random integers can be obtained by taking a series of values from this vector. Separate calls to RANDU, GGUBS, and VSRTP were made to pick each of the sets of 5, 15, and 30 seed profiles.

Subroutine RANDU requires a calling integer IX to return an integer to be used for the next call, IY, and a single random number. Taken collectively, the random numbers are distributed uniformly between 0 and 1.

```
SUBROUTINE RANDU (IX,IY,RAN)
IY=IX*65539
IF (IY) 5,6,6
5 IY=IY+2147483647+1
6 YFL=IY
YFL=YFL*.4656613E-9
RETURN
END
```

The numerical code for subroutine RANDU and function
ERFMI (Appendix C) was graciously provided by Dr. Henry
Fleming of the National Environmental Satellite Service.

APPENDIX C

GENERATION OF RANDOM ERRORS IN TEMPERATURE AND DEPTH

Simulated profiles were created by adding random errors to the randomly chosen seed profiles. Each error was determined by using separate calls to subroutine RANDU and function ERFM1. A call to RANDU (Appendix B) yielded a random number between 0 and 1. Function ERFM1 used this number as a calling argument to produce a random value from a normally distributed population with a mean of zero and a standard deviation of 1. By multiplying this value by the desired standard deviation, it was possible to create a random error from an error population which was normally distributed with a mean of zero and a standard deviation of the appropriate history window variable. Separate calls to RANDU and ERFM1 were made for the layer depth and for $T(Z)$, $Z = 1,199,2$. The process was repeated for each simulated profile.

```
FUNCTION ERFM1 (X)
Q=X
S=-1.0
IF (X-0.5) 2,2,1
1 Q=1.0-X
S=1.0
2 IF (Q) 3,3,4
3 Q=0.1E-05
4 ETA=SQRT(ALOG(1.0/(Q*Q)))
ETAS=ETA*ETA
ETAC=ETAS*ETA
AN=2.55517+.802853*ETA+.010328*ETAS
DN=1.0+1.432788*ETA+.189269*ETAS+.001308*ETAC
ERFM1=S*(ETA-AN/DN)
RETURN
END
```

BIBLIOGRAPHY

Anthes, Richard A., 1974: Data Assimilation and Initialization of Hurricane Prediction Models. J. Atmos. Sci., 31, 702-719.

Bjerknes, J., 1966: A Possible Response of the Atmospheric Hadley Circulation to Equatorial Anomalies of Ocean Temperature. Tellus, 18, 820-829.

Bjerknes, J., 1972: Large-scale Atmospheric Response to the 1964-1965 Equatorial Warming. J. Phys. Oceanogr., 2, 212-217.

Budd, Bruce W., 1980: Prediction of the Spring Transition and Related Sea Surface Temperature Anomalies. M.S. Thesis, Naval Postgraduate School, Monterey, CA, 1980.

Camp, N.T., and R.L. Elsberry, 1978: Oceanic Thermal Response to Strong Atmospheric Forcing. II. Simulations with Mixed Layer Models. J. Phys. Oceanogr., 8, 215-224.

Clancy, R.M., and P.J. Martin, 1980: Verification of a Synoptic Ocean Mixed Layer Model. Technical Report, Environmental Models Branch, Naval Ocean Research and Development Activity, NSTL Station, MS.

Elsberry, R.L., and N.T. Camp, 1978: Oceanic Thermal Response to Strong Atmospheric Forcing. I. Characteristics of Forcing Events. J. Phys. Oceanogr., 8, 206-214.

Elsberry, R.L., P.C. Gallacher, and R.W. Garwood, Jr., 1979: One-Dimensional Model Predictions of Ocean Temperature Anomalies During Fall 1976. Naval Postgraduate School Technical Report NPS 63-79-003, 30 pp.

Elsberry, R.L. and R.W. Garwood, Jr., 1978: Sea Surface Temperature Anomaly Generation in Relation to Atmospheric Storms. Bull. Am. Meteor. Soc., 59, 786-789.

Elsberry, R.L. and R.W. Garwood, Jr., 1979: First Generation Numerical Ocean Prediction Models - Goal for the 1980s. Naval Postgraduate School Technical Report NPS 63-79-007, 44 pp.

Gallacher, P.C., 1979: Preparation of Ocean Model Forcing Parameters from FNWC Atmospheric Analysis and Model Predictions. Naval Postgraduate School Technical Report NPS 63-79-005, 24 pp.

Gallacher, P.C., and R.W. Garwood, Jr., 1980: Schematic Description of the Garwood OPBL Model for Quasi-Steady State Conditions. Unpublished manuscript, Naval Post-graduate School, Monterey, CA.

Garwood, R.W., Jr., 1977: An Oceanic Mixed Layer Model Capable of Simulating Cyclic States. J. Phys. Oceanogr., 7, 455-468.

Garwood, R.W., Jr., and D. Adamec, 1980: Seventeen Years of Ocean Mixed Layer Simulation at Ocean Station PAPA. Unpublished manuscript, Naval Postgraduate School, Monterey, CA.

Hoke, James E., and Richard A. Anthes, 1976: The Initialization of Numerical Models by a Dynamic Initialization Technique. Mon. Wea. Rev., 104, 1551-1556.

McPherson, R.D., 1975: Progress, Problems, and Prospects in Meteorological Data Assimilation. Bull. Am. Meteor. Soc., 56, 1154-1166.

Namias, J., 1973: Thermal Communication Between the Sea Surface and the Lower Troposphere. J. Phys. Oceanogr., 3, 373-378.

Namias, J., 1976: Negative Ocean-Air Feedback Systems Over the North Pacific in the Transition from Warm to Cold Seasons. Mon. Wea. Rev., 104, 1107-1121.

Rowntree, P.R., 1972: The Influence of Tropical East Pacific Ocean Temperatures on the Atmosphere. Quart. J. R. Met. Soc., 98, 290-321.

INITIAL DISTRIBUTION LIST

	No. Copies
1. Defense Technical Information Center Cameron Station Alexandria, VA 22314	2
2. Library, Code 0142 Naval Postgraduate School Monterey, CA 93940	2
3. Dr. R.J. Renard, Code 63Rd Chairman, Department of Meteorology Naval Postgraduate School Monterey, CA 93940	1
4. Dr. C.N.K. Mooers, Code 68Mr Chairman, Department of Oceanography Naval Postgraduate School Monterey, CA 93940	1
5. Dr. R.L. Elsberry, Code 63Es Department of Meteorology Naval Postgraduate School Monterey, CA 93940	5
6. Dr. R.W. Garwood, Code 68Gd Department of Oceanography Naval Postgraduate School Monterey, CA 93940	1
7. Mr. P.C. Gallacher, Code 63 Department of Meteorology Naval Postgraduate School Monterey, CA 93940	1
8. Mr. David Adamec 5 Charles St. Putnam, CN 06260	1
9. Commanding Office (Attn: S. Piacsek) Naval Ocean Research and Development Agency NSTL Station, MS 39529	1
10. Commander Naval Oceanography Command NSTL Station, MS 39529	1

11.	LT L.L. Warrenfeltz, USN 965 Brookwood Dr. Pottstown, PA 19464	2
12.	Dr. R.L. Haney, Code 63Hy Department of Meteorology Naval Postgraduate School Monterey, CA 93940	1
13.	Director Naval Oceanography Division Navy Observatory 34th and Massachusetts Avenue NW Washington, D.C. 20390	1
14.	Commanding Officer Fleet Numerical Oceanography Center Monterey, CA 93940	1
15.	Commanding Officer Naval Environmental Prediction Research Facility Monterey, CA 93940	1
16.	Chairman, Oceanography Department U.S. Naval Academy Annapolis, MD 21402	1
17.	Commanding Officer Naval Oceanographic Office NSTL Station, MS 39529	1

DATE:
TIME